



Miguel Pedro Lopes Batista

Degree in Biology

Novel Alginate-Chitosan Aerogel Fibres For Potential Wound Healing Applications

Dissertation to obtain Master Degree in
Biotechnology

Supervisor: Vanessa Gonçalves, PhD, iBET
Co-supervisor: Frédéric Gaspar, PhD, iBET

Jury

President: Prof. Doutora Susana Filipe Barreiros
Arguer: Prof. Doutora Ana Rita Cruz Duarte
Supervisor: Doutora Vanessa Gonçalves



FACULDADE DE
CIÊNCIAS E TECNOLOGIA
UNIVERSIDADE NOVA DE LISBOA

September 2018

Novel Alginate-Chitosan Aerogel Fibres for Potential Wound Healing Applications
Miguel Batista





UNIVERSIDADE
NOVA
DE LISBOA



FACULDADE DE
CIÊNCIAS E TECNOLOGIA
UNIVERSIDADE NOVA DE LISBOA

Miguel Pedro Lopes Batista

Degree in Biology

Novel Alginate-Chitosan Aerogel Fibres for Potential Wound Healing Applications

Dissertation to obtain Master Degree in
Biotechnology

Supervisor: Vanessa Gonçalves, PhD, iBET
Co-supervisor: Frédéric Gaspar, PhD, iBET

Jury

President: Prof. Doutora Susana Filipe Barreiros
Arguer: Prof. Doutora Ana Rita Cruz Duarte
Supervisor: Doutora Vanessa Gonçalves

September 2018

“Copyright”

Novel Alginate-Chitosan Aerogel Fibres for Potential Wound Healing Applications

Miguel Pedro Lopes Batista, FCT/UNL e UNL

A Faculdade de Ciências e Tecnologia e a Universidade Nova de Lisboa têm o direito, perpétuo e sem limites geográficos, de arquivar e publicar esta dissertação através de exemplares impressos reproduzidos em papel ou de forma digital, ou por qualquer outro meio conhecido ou que venha a ser inventado, e de a divulgar através de repositórios científicos e de admitir a sua cópia e distribuição com objetivos educacionais ou de investigação, não comerciais, desde que seja dado crédito ao autor e editor.

Acknowledgments

A todos aqueles que direta ou indiretamente contribuíram para que esta etapa fosse alcançada, o meu profundo agradecimento.

Aos meus orientadores, à Vanessa e ao Frédéric, agradeço-vos por toda a confiança depositada e por todo o conhecimento que me transmitiram. A maneira como ambos pensam a ciência e a vossa capacidade multidisciplinar foram sem dúvida a inspiração que me orientou neste trabalho e me irá orientar para o futuro.

À Doutora Ana Matias agradeço a oportunidade de me ter permitido desenvolver este trabalho no grupo Nutraceuticals & Bioactives Process Technology. Deixar também uma palavra de profundo agradecimento a todos os membros deste grupo pela ajuda e companheirismo prestado. Um obrigado especial à Carolina e à Ana Roda pelo vosso apoio. À Doutora Teresa Crespo e a todos os membros dos grupos Food Safety & Microbiology e Membrane Processes pela vossa disponibilidade e boa disposição.

Ao Baixinho e ao Pedro, obrigado pela vossa presença e por todas as felicidades e tristezas partilhadas ao longo desta caminhada. Um profundo obrigado aos amigos de longa data Simão, Diogo, Pimentel, Louro, Salomé, Melo e David pelo vosso apoio e compreensão da minha ausência nos momentos mais atribulados. Aos grandes amigos de Coimbra, que mesmo longe se fizeram sentir sempre perto, obrigado Costa, Bibiana, Sandro, Cardoso e Daniel. Aos companheiros “lisboetas”, obrigado Sofia, Serafim, Tiago e Adriana, que me fizeram sentir menos deslocado nesta aventura.

Por fim, os meus últimos agradecimentos vão para a minha família. Aos meus pais, aos meus avós e ao meu irmão agradeço-vos profundamente por toda a ajuda na concretização desta etapa.

Abstract

Aerogels are very interesting materials with high porosity whose wound healing applications are arousing great interest. In particular, aerogels produced from marine polymers are of particular interest due to their attractive properties such as the antimicrobial activity of chitosan or the capacity to provide a moist environment of alginate. The aim of this work was to evaluate the potential for wound healing applications of alginate-chitosan aerogels in the form of fibres. To produce the fibres, a polyelectrolyte complex hydrogel of both polymers was made by the emulsion-gelation method. Through solvent exchange an alcogel was obtained which was then dried with supercritical CO₂. Once the fibres were produced, the characterization of its solid state, biocompatibility, cell migration stimulation and antimicrobial activity were carried out. To characterize the solid state, determination of the fibre's chitosan content was first performed. Then, the morphology, its textural properties and the ionic interaction between both polymers was also analysed. Fibres biocompatibility and stimulation of cell migration were evaluated by two *in vitro* methods, the direct contact method described in ISO 10993-5 and the scratch assay, respectively, using in both methods the mouse fibroblast NCTC clone 929 cell line. The antimicrobial activity was evaluated against *Staphylococcus aureus* and *Klebsiella pneumoniae* by two standard methods (dynamic and static) described in ASTM E 2149-01 and in ISO 20743:2013, respectively. In this work, the influence of chitosan's molecular weight and content on the fibre characteristics was also evaluated. In addition, in order to compare with a consumer product already on the market, cell and antibacterial assays were also performed for a dry calcium-sodium alginate wound dressing. The obtained results suggest that these alginate-chitosan aerogel fibres are good candidates for wound healing applications.

Keywords

Aerogel fibres; Alginate; Chitosan; Wound healing; Biocompatibility and cell migration; Antibacterial activity.

Resumo

Aerogéis são materiais muito interessantes com elevada porosidade, cujas aplicações em tratamento de feridas estão a despertar interesse. Particularmente, a produção de aerogéis a partir de polímeros marinhos apresentam particular interesse devido às suas propriedades atrativas, tais como a atividade antimicrobiana do quitosano ou a capacidade de proporcionar um ambiente húmido do alginato. O objetivo deste trabalho foi avaliar o potencial de aerogéis de alginato-quitosano na forma de fibras para aplicações em tratamentos de feridas. Para produzir as fibras, produziu-se um complexo polieletrólítico na forma de hidrogel entre os polímeros pelo método de emulsão-gelificação. Através do processo de troca de solvente foi obtido um alcogel o qual foi secado por CO₂ supercrítico. Assim que produzidas, realizou-se a caracterização do estado sólido, biocompatibilidade, estimulação da migração celular e atividade antimicrobiana das fibras. Para caracterizar o estado sólido, começou-se por determinar o conteúdo de quitosano. Em seguida, a morfologia, as propriedades texturais e a interação iónica entre os dois polímeros também foram analisadas. A biocompatibilidade e a estimulação da migração celular foram respetivamente avaliadas através de dois métodos *in vitro*, o método por contato direto descrito na ISO 10993-5 e o ensaio de migração celular, utilizando em ambos a linha celular de fibroblastos de ratinhos NCTC clone 929. A atividade antimicrobiana foi avaliada em *Staphylococcus aureus* e *Klebsiella pneumoniae* por dois métodos padrão (dinâmico e estático) descritos na norma ASTM E 2149-01 e na ISO 20743:2013. Neste trabalho também foi avaliada a influência do peso molecular e do conteúdo de quitosano nas características das fibras. Além disso, de modo a comparar com um produto de consumo já existente no mercado, os ensaios celulares e antibacterianos também foram realizados para um apósito de alginato de cálcio e de sódio. Os resultados obtidos sugerem elevado potencial destas fibras para aplicações em tratamentos de feridas.

Palavras-chave

Fibras de aerogel; Alginato; Quitosano; Cicatrização de feridas; Biocompatibilidade e migração celular; Atividade antibacteriana.

List of Contents

Acknowledgments	VII
Abstract	IX
Keywords	IX
Resumo	XI
Palavras-chave	XI
List of Contents	XIII
List of Figures	XV
List of Tables	XVII
List of Abbreviations	XIX
1. Introduction	1
1.1 Aerogels production	1
1.2 Aerogels from biopolymers	3
1.2.1 Alginate.....	4
1.2.2 Chitosan.....	6
1.2.3 Polyelectrolyte complexes.....	8
1.3 Biomedical applications of aerogels	10
1.3.1 Wound healing process.....	10
1.3.2 Wound dressings materials	11
1.4 Aim of the thesis	13
2. Materials and Methods	15
2.1 Aerogel fibres production	15
2.1.1 Reagents	15
2.1.2 Stock solutions	15
2.1.3 Sol-Gel process.....	15
2.1.4 Solvent exchange	16
2.1.5 Drying with supercritical carbon dioxide	16
2.2 Fibres weighing and sterilization	17
2.3 Solid-state characterization	17
2.3.1 Scanning electron microscopy (SEM)	17
2.3.2 Fourier-transform infrared spectroscopy (FTIR).....	17
2.3.3 Brunauer-Emmett-Teller (BET) surface area analysis and Barrett-Joyner-Halenda (BJH) pore size and volume analysis	18
2.3.4 Elemental analysis (EA)	18
2.4 Cell-based assays	18
2.4.1 Reagents	18
2.4.2 Cell culture.....	18
2.4.3 Biocompatibility – ISO 10993-5 <i>in vitro</i> cytotoxicity assay	19

2.4.4	Bioactivity - Scratch assay.	19
2.5	Antibacterial activity evaluation assays.....	20
2.5.1	Materials	20
2.5.2	Bacterial test species, bacterial suspensions and standardized inoculum preparation... ..	20
2.5.3	Well diffusion and agar plate methods	21
2.5.4	ASTM E 2149-01 standard test method for determining the antimicrobial activity of immobilized antimicrobial agents under dynamic contact conditions.	21
2.5.5	ISO 20743:2013(E) Textiles — Determination of antibacterial activity of textile products by absorption method.	21
2.5.6	Antimicrobial susceptibility testing by broth microdilution	22
2.6	Statistical analysis.....	23
3.	Results and Discussion	25
3.1	Screening and optimization of assays for evaluation of potential wound healing applications of alginate-chitosan aerogel fibres	25
3.1.1	Aerogel fibres production	25
3.1.2	Implementation of sterilization method.....	25
3.1.3	Implementation of cell culture.....	25
3.1.4	Optimization of cell-based assays.....	26
3.1.4.1	Biocompatibility – ISO 10993-5 <i>in vitro</i> cytotoxicity assay	26
3.1.4.2	Bioactivity - Scratch assay.....	26
3.1.5	Evaluation of antimicrobial activity: screening and assays optimization.....	26
3.1.5.1	Well diffusion and agar plate methods	26
3.1.5.2	Static method	26
3.1.5.3	Dynamic method	27
3.2	Evaluation of alginate-chitosan aerogel fibres for potential wound healing applications	27
3.2.1	Influence of chitosan molecular weight	27
3.2.2	Influence of chitosan content.....	34
4.	Conclusion	45
5.	References	47

List of Figures

Figure 1.1 - Main steps of the production process of an aerogel.	2
Figure 1.2 - Pressure versus temperature phase diagram of CO ₂ indicating the critical point and the sub- and super-critical regions [5].	2
Figure 1.3 - (a) Scheme of the forces exerted by the surface tension due to the interface of gas-liquid phases; (b) Effect of gel drying method: gel monoliths of pectin of the same dimensions prepared by thermal gelation dried under supercritical drying (aerogel) and under air drying (xerogel) [4].	3
Figure 1.4 - Representative alginate structure: G-block, M-block, and alternating MG-blocks in alginate [13].	5
Figure 1.5 - Structure of chitin and chitosan (reproduced from [22]).	7
Figure 1.6 - Schematic representation of polyanion-polycation interactions: mixing of the oppositely charged polyelectrolytes in aqueous solution leads to formation of a dense phase (PEC) caused by the cooperative electrostatic interactions between the ions [28], [31].	9
Figure 1.7 - Work plan for the present thesis organized in two main tasks.	13
Figure 2.1 - Schematic diagram of the supercritical fluid drying apparatus. (Adapted from Waters, 2010)	17
Figure 3.1 - Photographs of the aerogel fibres produced with different chitosan MW (low and medium).	27
Figure 3.2 - SEM micrographs of alg:chitLMW 99:1 (a,b) and alg:chitMMW 99:1 (c,d) aerogel fibres, at 2000x (a,c) and 30000x (b,d) magnification.	29
Figure 3.3 - FTIR spectra of (a) sodium alginate, (b) MMW chitosan and (c) LMW chitosan raw materials; (d) alg:chitMMW 99:1 and (e) alg:chitLMW 99:1 aerogel fibres.	30
Figure 3.4 - BET surface area (a) and BJH pore volume (b) of alg:chitLMW 99:1 and alg:chitMMW 99:1 aerogel fibres.	31
Figure 3.5 - Cytotoxicity assay using MTS reagent: samples (fibres and pure compounds) were incubated, at a concentration of 1.7 mg/mL, in NCTC clone 929 cell line during 24 h at 37°C and 5% CO ₂ humidified atmosphere (mean ± SD, n=3; except controls n=6). Solution of 10% (v/v) of DMSO in cell culture media was used as a positive cytotoxic control. If viability is reduced to <70% of the control, samples have a cytotoxic potential. Statistically significant differences comparing all conditions are indicated by **** (p < 0.0001).	32
Figure 3.6 - Percent reduction of <i>S. aureus</i> and <i>K. pneumoniae</i> resulting from contact with samples, at a concentration of 0.8 mg/mL, during 2.5 h at 37°C (mean ± SD, n=3; except controls n=6). Cotton disks were used as untreated control. Statistically significant differences observed between all fibre conditions are indicated by **** (p < 0,0001).	33
Figure 3.7 - Photographs of the aerogel fibres produced with different chitosan content.	35

Figure 3.8 - SEM micrographs of alg:chitLMW 99:1 (a,b), alg:chitLMW 19:1 (c,d) and alg:chitLMW 9:1 (e,f) aerogel fibres, at 2,000x (a,c,e) and 30,000x (b,d,f) magnification.	36
Figure 3.9 - FTIR spectra of (a) sodium alginate and (b) LMW chitosan raw materials; (c) alg:chitLMW 9:1, (d) alg:chitLMW 19:1 and (e) alg:chitLMW 99:1 aerogel fibres.	37
Figure 3.10 - BET surface area (a) and BJH pore volume (b) of alg:chitLMW 99:1, 19:1 and 9:1 aerogel fibres.	38
Figure 3.11 - Cytotoxicity assay using MTS reagent: samples were incubated, at a concentration of 1.7 mg/mL, in NCTC clone 929 cell line during 24 h at 37°C and 5% CO ₂ humidified atmosphere (mean ± SD, n=3; except controls n=6). Solution of 10% (v/v) of DMSO in cell culture media was used as a positive cytotoxic control. If viability is reduced to <70% of the control, samples have a cytotoxic potential. Statistically significant differences comparing all conditions are indicated by **** (p < 0,0001).	39
Figure 3.12 - Scratch assay: samples were incubated, at a concentration of 1.7 mg/mL, in NCTC clone 929 fibroblasts, during 8h at 37°C and 5% CO ₂ humidified atmosphere (mean ± SD, n=4). Statistically significant differences when compared to control conditions are indicated by **** (p < 0.0001).	40
Figure 3.13 - Percent reduction of <i>S. aureus</i> resulting from contact with samples, at a concentration of 0.8 mg/mL, during 2.5 h at 37°C (mean ± SD, n=3; except controls n=6). Cotton disks were used as untreated control. Statistically significant differences observed between all conditions are indicated by *** (at least p ≤ 0.0004).	41
Figure 3.14 - Percent reduction of <i>K. pneumoniae</i> resulting from contact with samples, at a concentration of 0.8 mg/mL, during 2.5 h at 37°C (mean ± SD, n=3; except controls n=6). Cotton disks were used as untreated control. Statistically significant differences observed between all conditions are indicated by **** (p < 0.0001).	41
Figure 3.15 - Percent reduction of <i>S. aureus</i> and <i>K. pneumoniae</i> resulting from contact with samples, at a concentration of 0.8 mg/mL, during 2.5 h at 37°C (mean ± SD, n=3; except controls n=6). Cotton disks were used as untreated control. Statistically significant differences observed between all fibre conditions are indicated by * (p < 0.05).	42

List of Tables

Table 1.1 - Examples of some of the commercial wound dressing materials.....	12
Table 2.1 - Mass of alginate and chitosan present in stock solutions used in fibre productions and final polymer ratio.	16
Table 3.1 - Chitosan content of alg:chitLMW (99:1) and alg:chitMMW 99:1 aerogel fibres; and respective chitosan raw materials used in their production.	28
Table 3.2 - Antimicrobial property efficacy of the tested material against <i>S. aureus</i> and <i>K. pneumoniae</i> from contact with samples, at a concentration of 2 g/mL, during 24 h at 37°C (mean \pm SD, n=3). Efficacy is defined as significant (for $2 \leq$ antibacterial value < 3), strong (for antibacterial value ≥ 3), or N/A (not applicable for values < 2).	33
Table 3.3 – Antimicrobial susceptibility testing of low and medium MW chitosans against <i>S. aureus</i> and <i>K. pneumoniae</i> . Median and triplicate values of MICs (mg/mL) are presented.	34
Table 3.4 - Chitosan content of alg:chitLMW 99:1, 19:1 and 9:1 aerogel fibres; and respective chitosan raw material used in their production.	35
Table 3.5 - Efficacy of antibacterial property of the tested material against <i>S. aureus</i> and <i>K. pneumoniae</i> from contact with samples, at a concentration of 2 g/mL, during 24 h at 37°C (mean \pm SD, n=3). Efficacy is defined as significant ($2 \leq$ antibacterial value < 3), strong (antibacterial value ≥ 3), and N/A (not applicable for values < 2).....	43

List of Abbreviations

Abbreviation	Full form
Alg	Alginate
ANOVA	Analysis of variance
AST	Antimicrobial susceptibility testing
BET	Brunauer–Emmett–Teller
BJH	Barrett-Joyner-Halenda
BPR	Back pressure regulator
CAMHB	Cation-adjusted Mueller-Hinton broth
Chit	Chitosan
CLSI	Clinical and Laboratory Standards Institute
DD	Degree of deacetylation
DMSO	Dimethyl sulfoxide
EA	Elemental analysis
EACC	European Collection of Authenticated Cell Cultures
EDTA	Ethylenediaminetetraacetic acid
FBS	Fetal bovine serum
FEG-SEM	Field emission gun scanning electron microscopy
FTIR	Fourier-transform infrared spectroscopy
G	Guluronate
GRAS	Generally recognized as safe
ISO	International Organization for Standardization
LMW	Low molecular weight
M	Mannuronate
MEM	Minimum essential medium
MHA	Mueller-Hinton agar
MIC	Minimal inhibitory concentration
MMW	Medium molecular weight
MTS	3-(4,5-dimethylthiazol-2-yl)-5-(3-carboxymethoxyphenyl)-2-(4-sulfophenyl)-2H-tetrazolium)

MW	Molecular weight
NA	Nutrient agar
NB	Nutrient broth
NCTC	National Collection of Type Cultures
NEAA	Non-essential amino acid
PBS	Phosphate buffered saline
PEC	Polyelectrolyte complex
SC-CO ₂	Supercritical carbon dioxide
SD	Standard deviation
SEM	Scanning electron microscopy
TSA	Tryptic soy agar
TSB	Tryptic soy broth
UV	Ultra violet
W/O	Water-in-Oil

1. Introduction

1.1 Aerogels production

Aerogels are a type of material which interest has increased in recent years. Discovered in the 1930's by Stephens Kistler, these innovative materials have gained considerable interest due to the unique combination of its properties. They have high porosity (~80–99.8%), low density (~0.003–0.5 g/cm³) and weight, low thermal conductivity, flexibility, high surface area (~200–1200 m²/g) and very low dielectric constant that give these materials a huge potential for applications in a wide spectrum of areas, ranging from construction, chemical engineering and more recently to life sciences and medicine [1]–[3].

An aerogel consists of an amorphous solid material resulting from a hydrogel, where the fluid of this gel is removed and replaced with a gas, keeping the gel structure almost intact, which results in its characteristic significant porosity [3]. It is the type of drying/extraction of the liquid phase of hydrogel that determines the formation of this innovative material. This drying can be performed through supercritical fluid technology, a methodology of compressed fluids that has revolutionized the extraction of various compounds, as well as the production of new materials such as aerogels [2], [4]. Prior to drying step, two steps are important in the production of an aerogel (Figure 1. 1). A first step relates to the formation of the hydrogel, usually starting from an aqueous solution. The gelation can be triggered by an action of physical or chemical nature. For example, physical hydrogel may refer to a reversible crosslink formed between polymeric chains under appropriate conditions through weak forces (e.g. hydrogen bonding or ionic interactions). Also, the gel induction through pH or temperature variations are some examples of mechanisms for the preparation of physical hydrogels [3], [4]. On the other hand, a chemical hydrogel may refer to wet gels obtained by establishing covalent bonds between polymeric chains mediated by the addition of chemical cross-linking agents [3], [4]. After obtaining the hydrogel, a second step before drying is performed. Since the drying is mostly done with supercritical carbon dioxide (scCO₂), the hydrogel solvent is exchanged for an organic solvent, usually ethanol because of its affinity for scCO₂ [3]. In carrying out this step, it must also be taken into account that the chosen organic solvent must be completely miscible in water, cannot displace the gel structure and must be done in several soft steps, as an aggressive change could lead to the collapse of the gel structure, reducing the characteristic porosity of the aerogel [4].

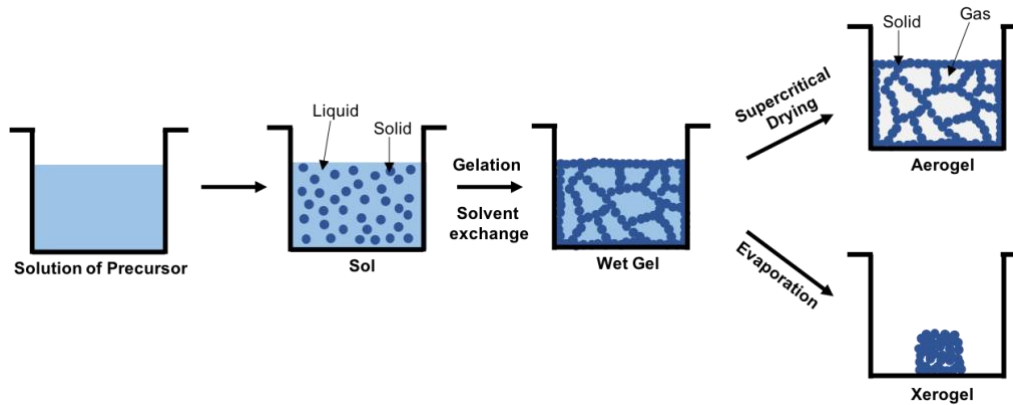


Figure 1.1 - Main steps of the production process of an aerogel.

As previously stated, the drying technique after the solvent exchange step is a critical factor in obtaining an aerogel. So, conventional drying techniques (e.g. air-drying and lyophilization) cannot be adopted since capillary forces from fluid evaporation can lead to the shrinkage of the initial structure, obtaining another type of dry gel much less porous, such as a xerogel. So, supercritical drying technology is used in order to avoid capillary forces, ensuring the structural integrity of the gel from which the aerogel results [3].

A supercritical fluid is understood as a substance that is at a temperature and pressure above its critical point, in which a phase separation between the liquid and gaseous states is not distinguished [3]. Among the various properties of supercritical fluid, its liquid-like density and its gas-like viscosity and diffusivity stands out [5]. Within the supercritical fluids, one of the most used is scCO_2 . A high number of properties make this gas one of the most used solvents in supercritical technology. Among them, the fact that it is a very abundant gas, non-toxic, non-flammable, economically cheaper, non-carcinogenic, and easily recyclable [6]. The pressure (73.8 bar) and specifically the temperature (31.1 °C) required to reach its critical point (Figure 1.2) are relatively close to ambient conditions, making this supercritical fluid one of the safest to operate [4].

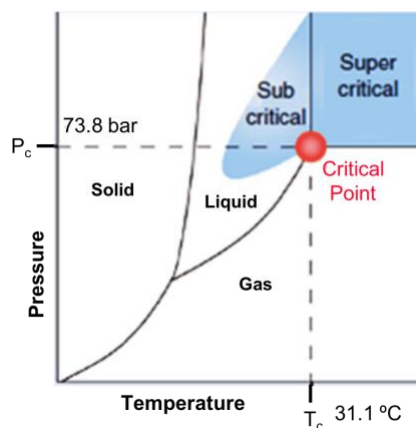


Figure 1.2 - Pressure versus temperature phase diagram of CO_2 indicating the critical point and the sub- and super-critical regions [5].

As previously stated, to produce an aerogel capillary forces must be avoided, so that the initial structure of the gel remains practically the same after solvent removal. This is why scCO_2 and ethanol are usually used in the production of aerogels. In Figure 1.1, a solvent exchange step is carried out in the production of an aerogel. This step is done so that the solvent present in the hydrogel has complete miscibility with scCO_2 , something that would not be possible with H_2O due to their miscibility gap [7]. The exchanged solvent is usually a low molecular weight (LMW) alcohol, which under certain pressure and temperature conditions achieves complete miscibility in the scCO_2 . For ethanol, miscibility in scCO_2 is assured at operating conditions of 120 bar and 40°C [2]. This creates the conditions that prevent capillary stress due to the absence of menisci liquid-vapor interface (Figure 1.3a), something that would happen if the gel was dried for example by evaporation, which would lead to shrinkage of the structure, resulting in a much less porous material like a xerogel [3] (Figure 1.3b).

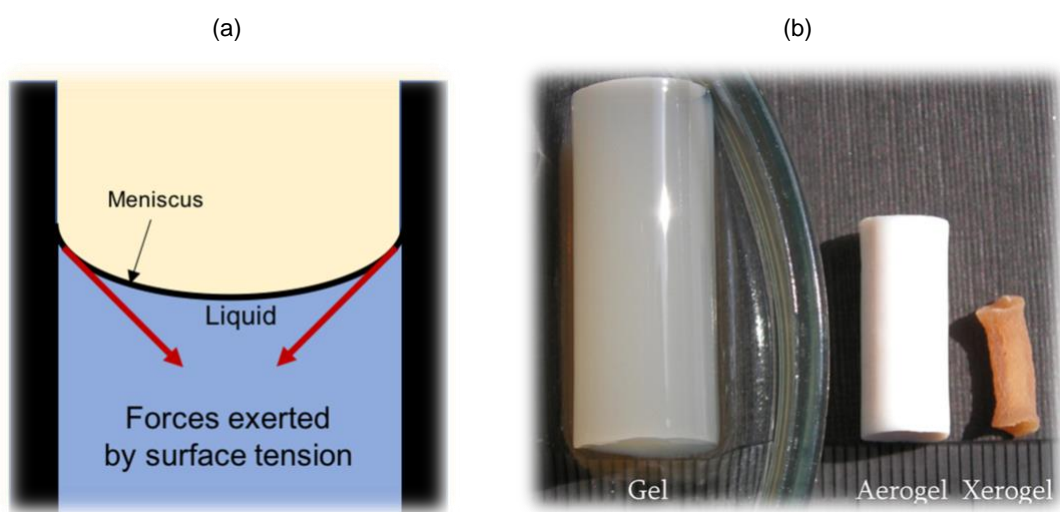


Figure 1.3 - (a) Scheme of the forces exerted by the surface tension due to the interface of gas-liquid phases; (b) Effect of gel drying method: gel monoliths of pectin of the same dimensions prepared by thermal gelation dried under supercritical drying (aerogel) and under air drying (xerogel) [4].

1.2 Aerogels from biopolymers

The most widely used classification of aerogels consists of three types based on their composition: inorganic, organic, and organic-inorganic hybrid aerogels [1]. The first aerogels produced were based on inorganic compounds such as silica, but new aerogels have emerged in recent years based on other compounds, such as polysaccharides. These compounds are classified as linear structures of bounded polymeric carbohydrates, which can be obtained from various organisms [8]. This class of biopolymers are allowing to obtain aerogels with properties that stand out from the conventional ones, or with enhanced characteristics like viscoplastic properties, comparing with the brittle nature of silica aerogels [2]. In addition, the characteristics of biopolymers themselves allowed to obtain aerogels with properties such as biocompatibility and biodegradability [4]. Some of these best-known polymers used in the production of aerogels are bacterial or plant cellulose, starch and pectin obtained from plants, alginate and agar from

algae, and chitin present in animals [4]. Within these various compounds, marine polysaccharides such as alginate and chitosan (deacetylated chitin) have gained prominence in aerogels production. There are already several studies where aerogels from these polymers have been produced, as is the case of Robitzer et al. [9] who explored the relationship at nanoscale of the polymer organization of alginate aerogel with its origin gel. Martins et al. [10] studied the potential of biomedical applications of alginate-based aerogels, evidencing the high potential of this materials, particularly for bone regeneration. Besides alginate, aerogels composed of other marine polymers are also emerging, such as the ones described in the work of Ayers et al. [11], who studied the synthesis and properties of chitosan-silica hybrid aerogels, and verified the low cytotoxicity of this material. These biopolymers stand out for their abundant sources, since they can be obtained through waste recovery from the food industry (chitosan) or through algae (alginate), one of the most abundant marine sources of polysaccharides that are easily cropped [12]. As such, there has been an increase in the economic and scientific interest of these biopolymers due to the abundant natural availability and their physicochemical and biological properties, which will be discussed below as well as the interaction between both polysaccharides.

1.2.1 Alginate

Alginate is an abundant natural polymer mostly obtained from brown algae, exerting structural function, giving mechanical strength and flexibility. This negatively charged polymer has gained increasing relevance in several areas such as biomedical sciences and engineering. This increase in interest is due to its vast properties such as biocompatibility, ease of gelation, low toxicity and relatively low cost [13], [14]. In an economy increasingly growing, it is important to respond to industrial needs and at the same time ensuring the resources sustainability. Therefore, it can be said that alginate is a resource that can be considered almost inexhaustible, since macroalgae can be easily collected cultivated.

Commercial alginate is mainly obtained from algae of the class *Phaeophyceae*, and despite being one of the most abundant marine polymer, it can be obtained from other sources such *Azotobacter* and *Pseudomonas* spp. (bacterial biosynthesis) [13]. The most common commercial form is water-soluble sodium alginate powder, which is obtained through few steps. To obtain alginate, located in the algae intercellular matrix, an alkaline extraction is carried out, resulting in an extract which is then filtered. The alginate present in the filtrate is precipitated and then converted into sodium alginate in a solvent in which the sodium salt is not dissolved. After these conversions and further purifications the water-soluble sodium alginate powder is obtained [15]. The fact that alginate can be obtained from different algae species reflects a different composition of alginate depending on its source, since alginate presents a relation between its structure and the function performed not only in different algae but also in different tissues of the same algae [14]. To overcome this variability, bacterial biosynthesis arises providing alginate with more standardized physical properties and more defined chemical structures. This process, technically possible although still economically unviable, is in development[16]. Unlike alginate derived from

marine algae, this type of production may allow the reduction in batch-to-batch variability. The pathway of alginate biosynthesis is generally divided into (1) synthesis of GDP-mannuronic acid precursor, (2) cytoplasmic membrane transfer and polymerization, (3) periplasmic transfer and modification, and (4) export through the outer membrane [16]. With the increasing knowledge of microorganisms' genetic regulation and the development of areas such as synthetic biotechnology, it may be possible to produce alginate with more uniform properties and with additional features.

Alginate is a linear copolymer, which is a polymer derived from more than one species of monomer, containing blocks of (1,4)-linked β -D-mannuronic acid (M) and α -L-guluronic acid (G) residues. The blocks are composed of homopolymeric regions of consecutive G residues (GGGGGG), consecutive M residues (MMMMMM), and alternating M and G residues (GMGMGM), termed G-, M- and MG-blocks respectively [15].

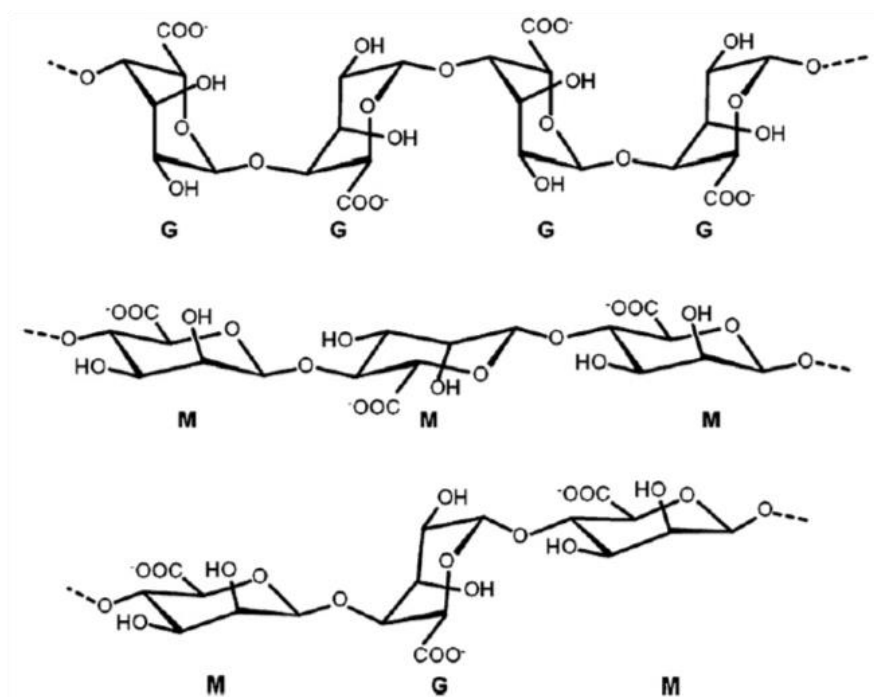


Figure 1.4 - Representative alginate structure: G-block, M-block, and alternating MG-blocks in alginate [13].

As stated above, the alginate composition may vary depending on its source, so the G and M contents of the commercial alginates may vary depending on their extraction source. The composition, sequence, and size of these residue blocks are critical factors that alter the physical properties of alginate [14]. Besides these characteristics, molecular weight (MW), ranging between 32,000 and 400,000 g/mol, is also a determining factor in the physical properties of commercial alginates[13].

Approved by the FDA as a compound that is Generally Regarded As Safe (GRAS), alginate has many applications. Due to its gelling ability under mild conditions and due to its stability, alginate

is widely used in the food industry as a thickener and emulsifier [17]. Alginate also has several properties that make it an excellent candidate for biomedical applications. The fact that it is a biocompatible polymer, does not present toxicity and is biodegradable makes this polymer ideal for human body direct applications [13]. The gelation ability is another interesting property for biomedical applications, since it allows the formation of hydrogels, microspheres, fibres, microcapsules and sponges [18]. These are different types of materials commonly used in biomedical applications such as wound healing, drug delivery and tissue engineering [13]. Another interesting property is that it presents a high bioadhesivity, comparing with other charged polymers, making this polymer an excellent candidate for drug delivery systems [17].

1.2.2 Chitosan

Chitin has a structural function similar to cellulose supporting cell and body surfaces and is mostly found in the exoskeleton of crustaceans, such as shrimp, crab and lobsters [19]. Chitosan, a polycationic polysaccharide, is also known as deacetylated chitin, and as such is considered a pseudonatural polymer. This cationic biopolymer presents a set of unique properties like biocompatibility, biodegradability and bioactivity that has greatly increased the interest of this polymer in biomedical applications [20]. Another interesting fact is that this polymer can be obtained through the waste recovery from food industry [19], an important aspect for the contribution to a circular economy, an essential concept for sustainable development.

Briefly, the chitosan obtaining process begins with the processing of the crustacean shells by removing calcium carbonate (decalcification) and proteins (deproteination) that are in large quantities. Chitin is then obtained, deacetylated using an alkaline solution, mainly of sodium hydroxide, for 1h-3h to give chitin with a deacetylation degree in the order of 70%, known as chitosan [21].

Chitin is a polymer of β -(1 \rightarrow 4)-linked N-acetyl-D-glucosamine and D-glucosamine units. It is the ratio between these units that defines the degree of deacetylation (DD) and which in turn defines if the polymer is chitin (DD < 0.5) or chitosan (DD > 0.5) [20]. DD is a very important factor from which the charge density, and consequently, the solubility of chitosan is highly dependent. Since the amine group has a pKa of \sim 6.5, at pH values < 6 occurs the protonation of the amine groups which make the chitosan positively charged and soluble in dilute acidic solutions [19]. In addition to DD, which normally ranges from 50-95%, also the MW, usually 10-1,000 kDa, purity and sequence of the amine groups are important parameters for the properties of chitosan [19].

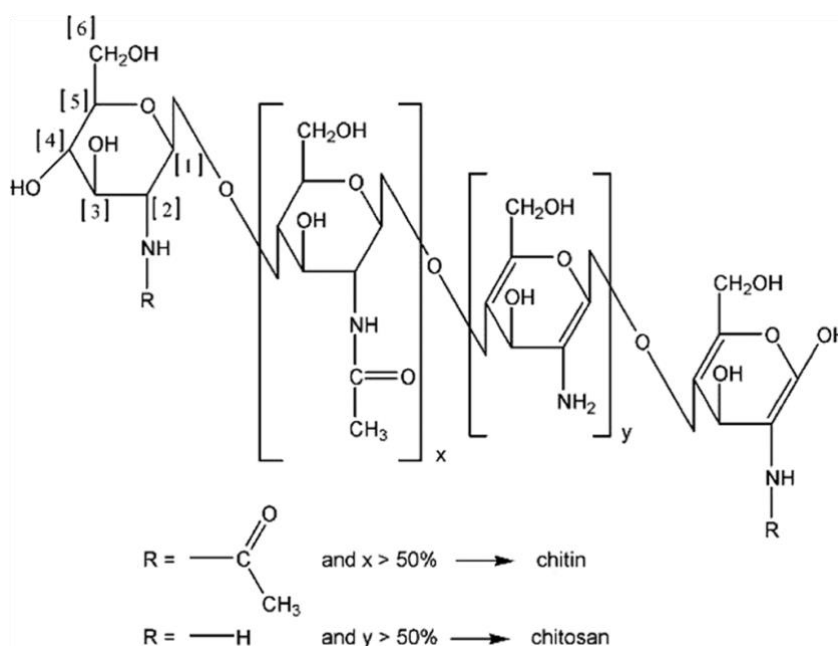


Figure 1.5 - Structure of chitin and chitosan (reproduced from [22]).

One of the reported properties of chitosan is its biodegradability. The occurrence of enzymes that catalyse its degradation, such as lysozyme, have been found from microorganisms to plants and mammals [23]. After several studies with ultrapure chitosan, from which toxic components and contaminants (e.g. heavy metals and proteins) were removed, its biocompatibility was confirmed. This fact contributed to FDA approving chitosan as GRAS [23]. One of the properties that most emphasizes chitosan is its antibacterial activity, being an important property that has taken the demand of this polymer in applications from food, textile or biomedical areas. The reported antibacterial activity of chitosan against a large number of microorganisms has greatly increased the interest of chitosan in biomedical applications such as tissue regeneration and wound healing, in order to control or reduce pathogens and preventing or eliminating severe infections in patients [24], [25]. However, in the literature there is still some variability of results regarding the antibacterial activity for the same organisms. This variability is due to a high set of factors on which the chitosan antimicrobial activity depends, beginning with the criteria used to evaluate and define the activity, as its own DD and MW, pH, ionic strength, presence of ionic metals, among others [23], [26], [27]. Also, haemostatic and antitumor activity, wound healing actions and immunological activity are reported in the literature, offering to this polymer an enormous potential in health areas [19], [20]. Unlike chitin, the fact that chitosan is soluble in acidic aqueous solutions allows the formation of hydrogels, another highly convenient property for the use of this polymer in biomedical applications. As such, chitosan has been used in the preparation of gels and other three-dimensional scaffolding materials such as fibres, films and sponges, for applications in areas such as tissue engineering, wound treatment or drug delivery systems [21], [23].

1.2.3 Polyelectrolyte complexes

Polyelectrolyte complexes (PECs) are the result of electrostatic interactions between polyions of oppositely charged polymers. The formation of PECs is directly related to contact, quantity and charge of both polyanionic and polycationic polymers [28]. Thus, the time, pH and temperature of interaction as well as the concentration and ratio of both polymers are important factors for the formation of these complexes. Another important factor is the distribution and density of positive and negative charges of both polymers, as well as their degrees of ionization [28]. Since electrostatic interactions are established between both polymers without the need of a chemical cross-linker agent, the PECs are generally non-toxic and biocompatible [29]. These complexes, in the form of hydrogels, microparticles or membranes, have gained considerable relevance in areas such as biotechnology and biomedicine, acting as drug delivery systems, biosensors, enzyme immobilizers or materials to aid bone and skin regeneration [28]–[30].

Alginate and chitosan are two polymers that well represent the phenomenon of the formation of PECs between two natural polymers. Alginate, as mentioned above, is a polyanionic polymer due to the presence of negatively charged carboxyl groups allowing electrostatic interactions with protonated amine groups of chitosan, a biopolymer positively charged in acidic medium. In addition to these electrostatic interactions, inter-macromolecular interactions may also occur, such as hydrophobic interactions, hydrogen bonds, dipole interactions and van der Waals forces, leading to the formation of a dense phase in aqueous medium without the need of chemical cross-linker agent [28], [29]. Depending on the alginate-chitosan content the anion-cation ratio is defined which may confer different characteristics and properties to this complex [29]. In Figure 1.6, the polyanion-polycation interaction between both polymers is schematized.

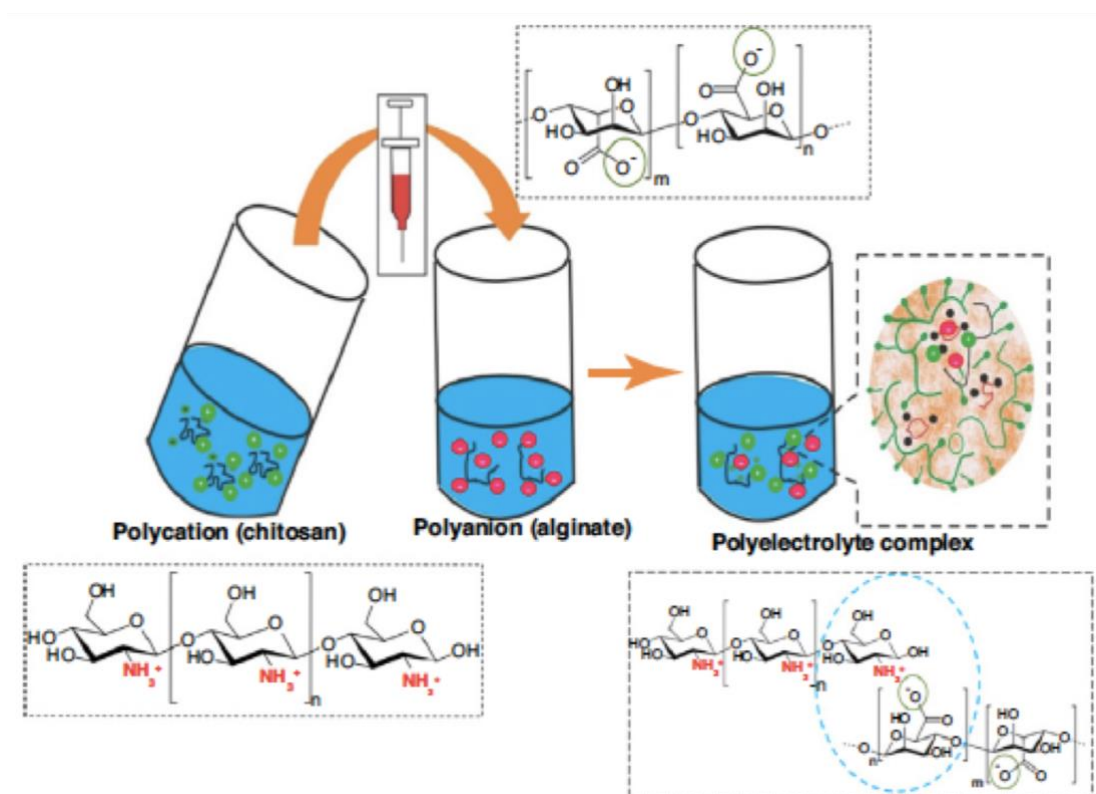


Figure 1.6 - Schematic representation of polyanion-polycation interactions: mixing of the oppositely charged polyelectrolytes in aqueous solution leads to formation of a dense phase (PEC) caused by the cooperative electrostatic interactions between the ions [28], [31].

Like for alginate or chitosan-only gels, the complex between both polymers also exhibits interesting physicochemical properties with potential biomedical applications. It is the example of the work of Liao et al. [32] that has demonstrated that the production of a PEC fibre of alginate-chitosan can be an effective drug carrier with potential advantages of high loading level and high encapsulation efficiency. Another study that demonstrated the biomedical potential of these materials was the one from Alsharabasy et al. [30], which demonstrated the preparation of a high quality alginate chitosan complex in the form of a hydrogel film that stimulates cell proliferation and wound closure, demonstrating the potentiality of these materials for wound healing applications.

As stated in the previous section (1.1), one of the steps required to obtain an aerogel is the formation of a hydrogel. Therefore, this is a step that can be achieved between alginate and chitosan because of these electrostatic interactions among both polymers forming PEC hydrogels, namely physical hydrogels, since a chemical cross-linker agent is not required for the induction of gel formation. As such, through supercritical drying technology, a biopolymer-based aerogel, composed of alginate and chitosan, can be obtained. This is a very interesting aspect due to the possible combination of the properties of the polymers themselves as well as of the aerogels. This possibility, coupled with the abundant natural source of these marine polysaccharides, arouses a high scientific and economic interest due to the high potential that this combination of characteristics may offer.

1.3 Biomedical applications of aerogels

The unique properties of the aerogels combined with the properties of the polymers that originate them, may offer numerous biomedical and pharmaceutical applications [1], [3]. Biocompatibility and biodegradability, as well as a good relationship between porosity and mechanical strength of aerogels obtained from biopolymers, are important properties for biomedical applications such as substrates for tissue regeneration, drug delivery systems, medical cardiovascular devices and wound care [1]–[3]. Among the various biomedical applications, the use of aerogels in the treatment of wounds has been an area that has also gained relevance.

1.3.1 Wound healing process

The skin, the largest organ of the human body, acts as a barrier against possible external aggressions, whether physical, chemical or even biological. It is an essential organ that goes through a very complex and highly regulated healing process when damaged [33]. When a severe aggression occurs, the tissue regeneration process must be highly accompanied by the responsible health professionals. This monitoring must be done in order to avoid complications such as the development of chronic non-healing wounds and serious infections that may even endanger the patient's life. Despite the improvement in medical care, there has been an increase in the development of this complications due to ageing and an increase in elderly population, as well as an increase in the prevalence of chronic diseases such as diabetes that affect the normal process of wound healing [34].

Briefly, the process of regeneration of damaged tissues occurs in three continuous phases: inflammatory, proliferative, and remodelling phase. The inflammatory phase begins shortly after temporarily restoring the barrier function of the injured tissue by haemostasis, where for a few minutes after the injury, the platelets of the leaked blood are activated and the polymerization of fibrin, a fibrous protein, occurs. Together, they form a wound protective clot. The aim of the inflammatory phase is to contain as much as possible the damaged location, beginning with the elimination of pathogens and material foreign to the wound [33]. At this stage occurs vasodilation and macrophages conversion, the cells responsible for phagocytosis of the wound exogenous elements [34], [35]. Fibroblasts begin to migrate to the wound giving rise to the proliferative phase, in which they synthesize collagen, one of the components of the extra cellular matrix, serving as support for the reepithelization of the epidermal tissues, thus closing the wound, the main objective of this phase. Angiogenesis also occurs, with endothelial cells creating new blood vessels in order to establish a vascular network that efficiently irrigates this very active zone due to the events of fibroplasia and granulation tissue formation [33]–[35]. Finally, the remodelling phase occurs, which can vary depending on the type and size of the initial wound. At this stage, tissue repair is achieved for its normal structure through the reorganization of extracellular matrix elements such as the synthesis of new collagen (type I) and removal of previously produced

collagen (type III) [34]. All cells that are no longer needed, such as endothelial cells from the vascular vessel network, are also removed and scar tissue formation occurs.

Wounds may assume various classifications, with respect to time, depth or type of injury. In relation to time, wounds with less than 6 hours are classified as acute. When the injury occurred more than 6 hours ago, but less than 5 days, are classified as subacute. After 5 days all wounds are chronic. According to the depth, they can be superficial, deep dermal or full thickness wounds. The type of wound may be due to incision, shearing, crushing or burning and consequently each of them can also be classified as sterile or contaminated [36]. The greatest and challenging dilemma of wound healing are the chronic non-healing wounds, as they mean that the normal healing process has been disturbed, leading to very severe complications such as severe infections and great tissue losses [24]. Among the chronic wounds are highlighted as clinically most frequent the pressure ulcers, diabetic ulcers, venous and arterial ulcers [37].

Wound contamination is a factor that requires a lot of concern since it can lead to one of the most serious complications of skin lesions. In a first "phase" the existence of non-replicative microorganisms in the wound is defined as contamination. However, an open wound means that the skin has lost its barrier ability and as such the wounds are colonized, where the adherent microorganisms gain the ability to replicate [38]. Yet, this is a state where there are no tissue losses. Due to a number of factors, such as the microorganism's concentration, their pathogenicity and virulence, and the response ability/inability of the host immune system to attack them, favourable conditions to the microorganism growth can be established. This microorganism replicative state may begin to cause damage to the patient's tissue, known as wound infection [38]. From this moment, if the infection is not controlled and eliminated, the spreading can lead to life-threatening conditions such as septicaemia. There are several skin commensal and wound colonizer microorganisms reported as potentially pathogenic, with *Staphylococcus aureus* and *Klebsiella pneumoniae* being two examples of commensal and nosocomial microorganisms commonly isolated from noninfected and infected wounds [38], [39].

1.3.2 Wound dressings materials

The treatment of wounds is an area that has gained a lot of interest from the scientific, medical and industrial communities. For medical device companies, it has been a market that has increased its attractiveness since it involves a large financial dimension around the world, with an annual market for wound care products estimated at \$15.3 billion [40]. An increase in the number of advanced and innovative wound dressings is emerging in the market. Nonetheless, they are still somewhat costly, making them less medically prescribed. However, since they accelerate the healing process and require less dressing changes than conventional products, it could make them less expensive in the future [24].

Traditional wound dressing products including gauze, plasters and cotton wool are used as a protective barrier for wounds to prevent contamination and exogenous material. However, in recent years polymeric wound dressings have been developed with the ability to play a more

active role in the wound healing process [37]. These advanced wound dressings have emerged as bioactive drug delivery systems, or wound dressings whose own polymeric material is already bioactive, capable of triggering the acceleration of healing and eliminating or hindering the development of infections [37]. In addition, these new wound dressings stand out from the traditional due to the creation of a moist environment (ideal for favouring the wound healing process) and a much less painful and easier of removal [41], [24]. There are already several types of commercial wound dressings made up of polymers that can be natural, synthetic or semi-synthetic (Table 1.1). Among the natural ones, some of the most used polymers are alginate, bacterial cellulose and pectin. Polyurethane and polyvinyl alcohol are commonly used synthetic polymers [37]. These types of new polymeric wound dressing materials can be classified regarding formulation or final form. Some of the examples are hydrogels, hydrocolloids and alginates which can be presented in the form of films, foam sheets, membranes or gels. In addition to these advanced wound dressing materials, aerogels are also gaining relevance in this type of applications. The high porosity of these materials presents as prominent property in the maintenance of gaseous exchanges essential for the normal wound healing process. Besides that, aerogels from some polysaccharides, in addition to biocompatibility and biodegradability, also present antimicrobial activity, high water uptake capacity and adhesive nature. Considering the complex process of wound healing, these characteristics make these materials very promising for possible wound care applications [1], [4], [12].

Table 1.1 - Examples of some of the commercial wound dressing materials.

Product name	Wound dressing description	Manufacturer
Granuflex®	Hydrocolloid composed of sodium CMC, gelatine and pectin	ConvaTec
Intrasite* Gel	Hydrogel composed of a modified CMC and propylene glycol	Smith & Nephew
Kaltostat®	Calcium/Sodium Alginate Dressing	ConvaTec
Lyof foam®	Polyurethane Foam	Mölnlycke Health Care
Sorbsan Flat	Non-woven Calcium Alginate	Aspen Medical

CMC – Carboxymethylcellulose

1.4 Aim of the thesis

The main objective of the present work was to evaluate the potential of new alginate-chitosan aerogel fibres, for applications in wound treatment.

To achieve the proposed aim, the work was divided in two fundamental tasks (Figure 1.7). In a first step the objective was to optimize the fibres production process, and to perform a previous screening of some fibre's properties. In addition, the purpose of this first step of the work was to optimize and implement the chosen methodologies and techniques to characterize the aerogels. The solid-state, biocompatibility and bioactivity of the fibres were chosen to be characterized.

After the first step, the methodologies were implemented to characterize the fibres in terms of chitosan content, morphology, textural properties, ionic interaction between both polymers, cytotoxicity, cell migration stimulation and antimicrobial activity. In addition to evaluating the fibres potential in this biomedical application, another objective was to evaluate the influence of aerogel chitosan content and its MW. In the second step the objective was then to produce the fibres, characterize their chosen properties and thus evaluate the influence of chitosan content and MW on the produced fibres characteristics.

This alignment will allow to achieve the main objective of this work, evaluate the potential of new alginate-chitosan aerogel fibres for wound healing applications.

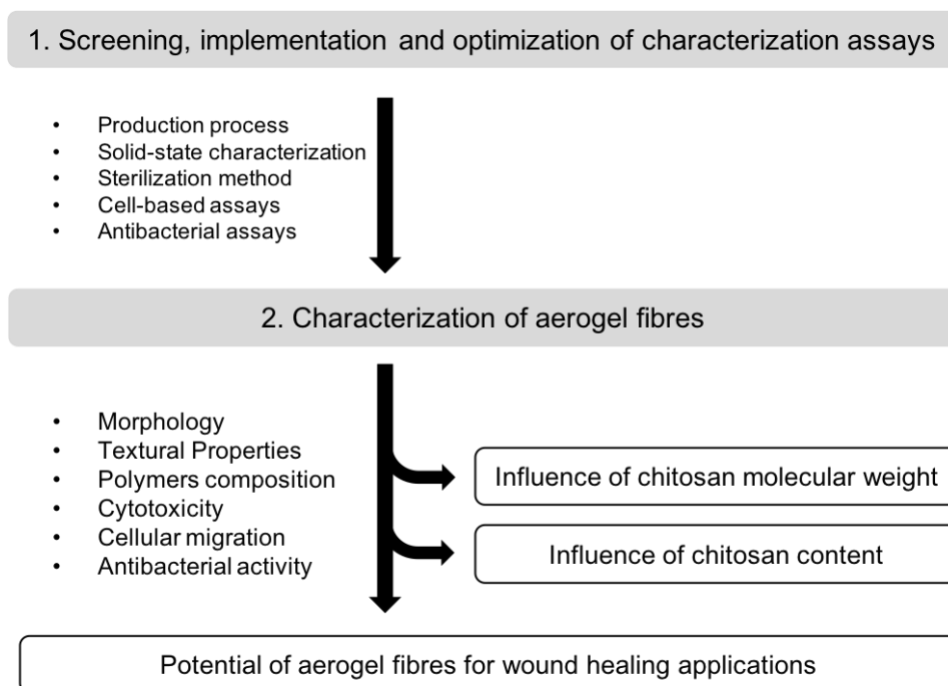


Figure 1.7 - Work plan for the present thesis organized in two main tasks.

2. Materials and Methods

2.1 Aerogel fibres production

The process described below was the same for all aerogel fibres production, only varying the amount of chitosan stock solution added to the alginate emulsion. Each production was done in duplicate, in two independent assays.

2.1.1 Reagents

Alginic acid sodium salt (90.8-106%) and acetic acid ($\geq 99.7\%$) were purchased from Panreac (Germany). LMW (50-190 kDa, 75-85% deacetylated, viscosity 20-300 cP) and medium molecular weight (MMW) (190-310 kDa, 75-85% deacetylated, viscosity 200-800 cP) chitosans were purchased from Sigma-Aldrich (Steinheim, Germany). Sorbitan monooleate (Span 80) was purchased from Merck (Germany). Paraffin oil was purchased from LabChem (USA). n-Hexane was purchased from Carlo Erba (Spain) and Ethanol ($\geq 99.8\%$, absolute) was purchased from Fisher Chemical (USA).

2.1.2 Stock solutions

For the emulsion production, the aqueous phase, an aqueous solution of sodium alginate (3 wt.%), was previously prepared by continuous stirring overnight at room temperature. The oil phase was produced by mixing paraffin oil with surfactant Span 80 (3 wt.%). In addition, acidic solutions of LMW and MMW chitosan (1.5 wt.%) were also prepared by dissolving chitosan in acetic acid (50% v/v) by continuous stirring overnight at room temperature.

2.1.3 Sol-Gel process

An Water-in-Oil (W/O) emulsion was made, adding slowly the aqueous phase, sodium alginate stock solution to the oil phase stock solution and then mixing with Ultra-Turrax homogenizer (T25, Ika Works Inc., USA) for 2 min at 24,000 rpm to provide energy to the system, facilitating the dispersion and homogenization [42]. The emulsions were always produced in the same W/O ratio (1:3 w/w).

In order to form an alginate hydrogel, the chitosan solution was added very slowly to the emulsion previously produced, stirring for 1 h at 800 rpm (Mechanical stirrer RW20.n IKA, Labortechnik, Germany) and finally allowed to stand overnight to complete the gelation. Table 2.1 shows the quantity of alginate and chitosan used to produce the fibres, as well as the resulting polymers ratio.

Table 2.1 - Mass of alginate and chitosan present in stock solutions used in fibre productions and final polymer ratio.

Aerogel Fibres (w/w)	Alginate (g)	Chitosan (g)
alg:LMWchit (99:1)	3	0.03
alg:MMWchit (99:1)	3	0.03
alg:LMWchit (19:1)	3	0.16
alg:LMWchit (9:1)	3	0.33

2.1.4 Solvent exchange

After overnight rest period, separation of phases occurred in the emulsion; consequently, top oil phase was removed by aspiration, followed by a centrifugation at 3583 g for 30 min with another removal by aspiration. To remove the remaining paraffin oil from the hydrogel, hexane was added to the centrifugation vial, stirred vigorously and centrifuged at 1593 g for 20 min removing the top liquid layer by aspiration (this step was done twice). For the solvent exchange, remaining suspension was rinsed with ethanol/water mixtures (30, 60, 90 and 100 vol.%) followed by centrifugation (1593 g, 20 min) and aspiration of the supernatant. Finally, to ensure water removal, this step was repeated three times with absolute ethanol. Centrifugations were done using a Beckman Coulter Avanti J-26 XPI centrifuge, a Beckman JA-10 rotor and Beckman 500mL centrifuge tubes. After solvent exchange, the alcogels were placed in filter papers which were stapled and placed in vials immersed in pure ethanol.

2.1.5 Drying with supercritical carbon dioxide

The alcogels were dried through scCO₂, using the high-pressure laboratory equipment (Thar Technology, Pittsburgh, PA, USA, model SFE-500F-2-C50), whose scheme is shown in Figure 2.1. Some glass beads were placed on the bottom of the drying vessel to facilitate the contact and diffusion of scCO₂ through the alcogel matrix. The coffee filters with the alcogels were placed inside the extraction vessel with more glass beads, to fully occupy its volume, and pure ethanol to avoid the alcogels drying by atmospheric air before the supercritical CO₂ drying process started. The pressurization of the vessel until 120 bar was performed in the following conditions: vessel heater at 40°C, heat exchanger at 40°C, CO₂ pump at 40 g/min and back pressure regulator (BPR) at 120 bar.

When the vessel pressure was reaching 120 bar, the CO₂ pump flow rate was decreased, and the drying was maintained in a CO₂ flow range of 8-12 g/min for 4 h. At the end the vessel was slowly depressurized, reducing BPR pressure very gradually to 0 bar and the fibres were stored inside a desiccator.

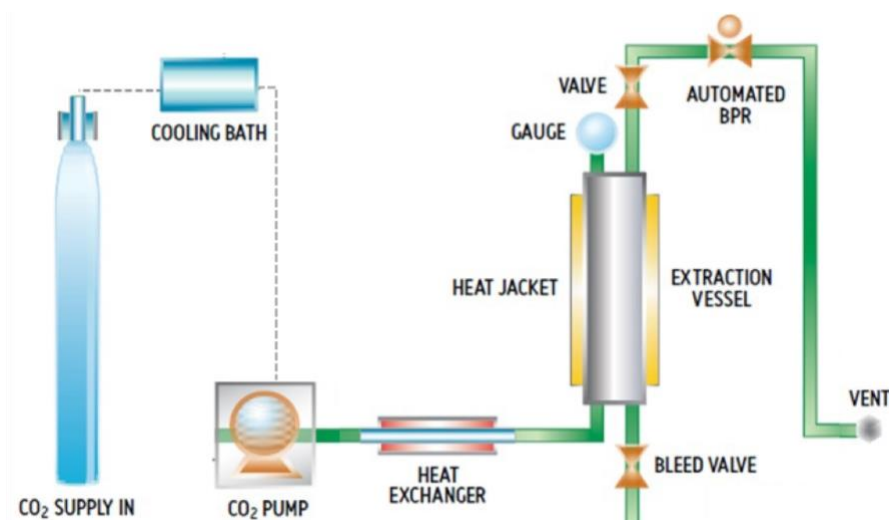


Figure 2.1 - Schematic diagram of the supercritical fluid drying apparatus. (Adapted from Waters, 2010)

2.2 Fibres weighing and sterilization

Since the sterility of medical devices used in wound healing treatment is required, aerogel fibres produced in this work were also subjected to sterilization process [43]. This will also guarantee their sterility in all cell and bacterial assays performed. The sterilization was performed using ultraviolet (UV) irradiation as already referenced in the literature [44], with some modifications. The sample mass required for each assay was previously weighed in petri dishes and then sterilized through exposure to the UV lamps of a Biological Safety Cabinets for 4 h (± 1 h) at room temperature. After exposure, a sterility test was performed to confirm the efficacy of the procedure. The aerogel fibres were incubated in Tryptic Soy Broth (TSB, Scharlau, Spain) at 37°C for 3 days. After 3 days, to ensure the absence of residual contamination, the suspension was plated in Tryptone Soya Agar (TSA, Oxoid, UK) for 24 h at 37°C. The material was considered sterile when no turbidity was observed after the TSB incubation and no microbial growth was observed on the TSA plates.

2.3 Solid-state characterization

2.3.1 Scanning electron microscopy (SEM)

Field Emission Gun Scanning Electron Microscopy (FEG-SEM) (JEOL, model JSM7001, Japan) was used to examine morphology. The samples were prepared for observation by covering with gold/palladium (Au/Pd), in a sputter coater (Quorum Technologies, model Q150TES). Micrographs of the prepared aliquots were taken at an acceleration voltage of 10 kV.

2.3.2 Fourier-transform infrared spectroscopy (FTIR)

The equipment used was a Thermo Scientific FTIR spectrometer (San Jose, USA) Class 1 Laser Product Nicolet 6100 using ATR accessories with a diamond crystal of 42° for solids. The acquisition of the spectra was performed using the software OMNIC version 7.3 (Thermo Electron

Corporation). The background spectrum of the air was collected before each sample spectrum acquisition. To clean the crystal, water and acetone were used and after that the crystal was dried with a soft tissue. For the sample spectrum acquisition, the different samples were placed in the corresponding ATR crystal and the spectra were recorded with 32 scans between 4,000-650 cm⁻¹ and with a resolution of 4 cm⁻¹.

2.3.3 Brunauer-Emmett-Teller (BET) surface area analysis and Barrett-Joyner-Halenda (BJH) pore size and volume analysis

Specific surface area and pore volume were determined by low temperature nitrogen adsorption desorption analysis (Quantachrome Nova 3000e) using Brunauer–Emmett–Teller (BET) and Barrett Joyner–Halenda (BJH) methods, respectively. Prior to the measurements, the samples were degassed at 348 K for 24 h. The results are presented as the mean values of two independent production processes.

2.3.4 Elemental analysis (EA)

The percentage of nitrogen content in the aerogel fibres was quantified by elemental analysis using a Thermo Finnigan Flash EA 1112 CHNS. The samples were weighed 2-3 mg and the total time of analysis was 12 min. The nitrogen content was converted to chitosan content (on a weight percentage basis, wt.%), as described in the literature [45], [46]. Calculated as follows:

$$\text{Chitosan (wt. \%)} = \frac{N(\text{wt. \%}) \times C(\text{g/mol})}{N(\text{g/mol})} \quad (\text{Eq.1})$$

This calculation is based on the weight percentage of nitrogen in the fibres, N (wt.%), determined by elemental analysis; the average MW of chitosan, C (g/mol), used to produce the fibres (considering the deacetylation degree) and the MW of elemental nitrogen, N (g/mol).

2.4 Cell-based assays

2.4.1 Reagents

Minimum essential medium (MEM) with Earle's balanced salts and 2.0 mM L-glutamine, phosphate buffered saline (PBS) and dimethyl sulfoxide (DMSO) were purchased from Sigma (USA). Non-essential aminoacids (NEAA), foetal bovine serum (FBS) and 0.25% (w/v) Trypsin-EDTA were purchased from Gibco (Life Technologies, USA). Aqueous One Solution Cell Proliferation Assay (MTS) was purchased from Promega (USA).

2.4.2 Cell culture

Mouse fibroblasts NCTC clone 929 (ECACC 88102702) cells were purchased from European Collection of Authenticated Cell Cultures (EACC, Public Health England, Salisbury, UK). Cells were routinely grown in a standard medium MEM supplemented with 1% NEAA and 10% heat-inactivated FBS. Stock cells were maintained as monolayers in 75 cm² culture flasks, cultured every week (seeding 30,000 cells/cm²) and incubated at 37°C in a 5% CO₂ humidified atmosphere. For cell passage, the cells were detached when confluence reached about 80%

using 0.25% trypsin/EDTA at 37°C. The cells were collected, and viability was determined using standard trypan blue staining procedure. Cell counting was performed using a haemocytometer. All cellular assays described below were performed with cells between passages 10 and 25.

2.4.3 Biocompatibility – ISO 10993-5 *in vitro* cytotoxicity assay

In order to mimic the contact of the fibres with skin cells, the aerogel fibres biocompatibility was evaluated by the direct contact method described in ISO 10993-5, a highly sensitive test of medical devices toxicity [47]. Cell viability was quantified through MTS cytotoxicity test, an assay based on the bio-reduction of the MTS tetrazolium compound by viable cells to generate a formazan dye that is soluble in cell culture media. The quantity of formazan dye, directly proportional to the number of living cells in culture, was quantified by measuring the absorbance at 490 nm.

NCTC clone 929 cells were seeded into 24-well plates (volume of 0.6 mL) with a density of 3.0×10^4 cells/cm² and maintained in culture for 24 h (~1 doubling period) to form a semi-confluent monolayer. This incubation period ensures cell recovery, adherence and progression to exponential growth phase. After 24 h, new MEM supplemented with 0.5% FBS was replaced, and following the direct contact method, cells were incubated for 24 h with 1 mg of sample per well, giving a final sample concentration of 1.7 mg/mL. The concentration used in this test was close as possible to the concentration used in the ASTM E 2149 assay, described below. Lastly, the culture media was removed, cells were rinsed with PBS and incubated for 2 h with 0.6 mL of MTS reagent assay, diluted according to the manufacturer's information. The absorbance was recorded at 490 nm using a microplate spectrophotometer (EPOCH, 219 Bio-Tek, USA). Experiments were performed in triplicate in three independent assays. The positive control of cytotoxicity was done with a treatment of 10% (v/v) DMSO solution diluted in MEM.

Results were expressed in terms of percentage of cellular viability (Viab.%) relative to control (cells without aerogel fibres). The lower the Viab.% value, the higher the cytotoxic potential of the test item is. Cytotoxic effect was considered for viability percentage below 70%, according to ISO 10993-5.

2.4.4 Bioactivity - Scratch assay.

One of the key steps in the wound healing process is the migration of fibroblasts initiating the proliferative phase [35], and as such, the *in vitro* scratch assay mimicking cell migration during wound healing was adopted. In this assay an image was captured after conducting a "scratch" in a cell monolayer. After a certain time interval (or regular intervals) the same area is again recorded to compare and quantify the migration rate of cells [48]. The migration assay was performed with the same cell line, seeding and sample concentration of the cytotoxicity assay. The plate wells were previously marked with a pen to help picture acquisition always in the same region.

NCTC clone 929 cells were seeded into 12-well plates (volume of 1.1 mL) and incubated for 48 h at 37°C, 5% CO₂ in order to reach a confluent cell monolayer. After the incubation period, with a

p200 pipette tip the cell monolayer was scratched in a straight-line crossing from one side of the well to the other creating the "scratch". The wells were then rinsed twice with PBS to remove all the suspension cells and freshly new MEM supplemented with 0.5% FBS was replaced. The samples were added and incubated for 8 h at 37°C in a 5% CO₂ humidified atmosphere. The same scratch area was captured at time point 0 h and 8 h, by microscope (Olympus CKX41) with a 4X objective, equipped with OPTIKAM 4083.B5 microscopy digital USB camera operated with OptikaSview software. Measurement of the wound area was manually calculated using Fiji software (ImageJ) and the results were expressed in terms of percentage (%) of wound recovery, calculated as follows:

$$\text{Wound recovered (\%)} = \frac{(A_{t=0h} - A_{t=8h})}{A_{t=0h}} \times 100 \quad (\text{Eq. 2})$$

Where,

$A_{t=0h}$ is the mean value of the measured area at t=0 h;

$A_{t=8h}$ is the mean value of the measured area at t=8 h.

2.5 Antibacterial activity evaluation assays

2.5.1 Materials

The growth media used in the tests described below were TSB, TSA, Nutrient Broth (NB, Oxoid, UK), Nutrient Agar (NA, Oxoid, UK), cation-adjusted Mueller Hinton Broth (CAMHB, BD Difco, USA) and Mueller Hinton Agar (MHA, BD Difco, USA). Working buffer solution (0.3 mM KH₂PO₄) was made dissolving PBS Tablets – Calbiochem (Merck, Germany) in distilled water. Saline solution was made dissolving (0,85% w/v) Sodium Chloride (Panreac, Spain) in distilled water. Kaltostat® was purchased from ConvaTec (UK). McFarland Standard 0.5 (Pro Lab Diagnostics, UK) was used as a reference to adjust the turbidity of bacterial suspensions. Antibiotic test discs (Fisher Scientific, EU) were used as untreated samples. All solutions were heat sterilized at 121°C for 15 min (moist heat sterilization).

2.5.2 Bacterial test species, bacterial suspensions and standardized inoculum preparation

Staphylococcus aureus ATCC 6538 (WDCM 00193) and *Klebsiella pneumoniae* CECT 8453 (WDCM 00192) were the strains selected as representative of gram-positive and gram-negative species, respectively. These species are recognized as skin commensals as well as nosocomial pathogens [38], [39] and are used as the test bacteria in ISO 20743:2013(E), one of the methods adopted in this work. The bacterial suspensions used in the methods described below were grown in 100 ml Erlenmeyer flasks with 20 ml of TSB or NB for *S. aureus* and *K. pneumoniae*, respectively, incubated at 37°C under agitation for 18 h to 24 h. Inoculum standardizations were prepared by diluting the overnight suspension in saline solution to achieve a turbidity equivalent

to a 0.5 McFarland standard ($\sim 1.5\text{-}3.0 \times 10^8$ CFU/ml). All antimicrobial activity assays described below were performed with both species.

2.5.3 Well diffusion and agar plate methods

The antimicrobial activity of the fibres was tested by two diffusion methods. The well diffusion assay was performed by adapting the Disk Diffusion Test CLSI M02-A11 guidelines [49]. The agar plate method was performed according to AATCC Test Method 90-2016 guidelines [50].

2.5.4 ASTM E 2149-01 standard test method for determining the antimicrobial activity of immobilized antimicrobial agents under dynamic contact conditions.

To measure the antimicrobial activity by the Flask-Shake Method (ASTM E 2149-01), hereon mentioned as dynamic method, all samples (aerogel fibres, Kaltostat® and the control fabric cotton disks) were prepared by weighing 40 mg and sterilizing as mentioned before (2.2). The working bacterial solution was prepared by diluting a standardized inoculum (2.5.2) into sterile working buffer solution in order to obtain a final concentration of $\sim 1.5\text{-}3.0 \times 10^5$ CFU/ml. Briefly, the working bacterial solution (50 ± 0.1 ml) was added to a sterile 250 ml Erlenmeyer. Once this step was done, the bacterial concentration of each flask was determined by performing serial dilutions and standard plate count techniques, defining the 0 h contact time. The samples were then placed in the flasks and incubated under orbital shaking (180 rpm) for 2.5 h. At the end of this period, the bacterial concentration of each flask was determined as was done for the 0 h contact time subgroup. Each assay included an inoculum only control and an untreated fabric control that were processed in the same way as each sample. The percent reduction of the organisms resulting from contact with the specimen was calculated using the following formula:

$$\text{Reduction, \% (CFU/mL)} = \frac{B-A}{B} \times 100 \quad (\text{Eq. 3})$$

Where,

A = CFU per millilitre for the flask containing the treated specimen after 2.5 h contact time;

B = CFU per millilitre for the flask used to determine “A” before the addition of the treated specimen (0 h contact time).

2.5.5 ISO 20743:2013(E) Textiles — Determination of antibacterial activity of textile products by absorption method.

The antibacterial performance of the aerogel fibres was also measured using the absorption method from ISO 20743:2013(E), hereon mentioned as static method. All samples (aerogel fibres, Kaltostat® and the control fabric cotton disks) were prepared weighing 40 mg and sterilizing as mentioned before (2.2). Briefly, 0.4 ml of each standardized inoculum (2.5.2) were transferred to 20 ml of fresh broth media and incubated at 37°C, under agitation for 3 h. The 3 h culture was then serially diluted in 20x water diluted broth media at room temperature, adjusting the bacterial concentration to $1\text{-}3 \times 10^5$ CFU/ml. For both target bacteria, two vials of each sample were

prepared for both contact time (0 h and 24 h). All vials containing the samples were inoculated with 20 µl of the previously adjusted bacterial suspension ($1-3 \times 10^5$ CFU/ml) in order to allow it to be fully absorbed. Following the inoculation step, to one vial of each sample was added immediately 2 ml of shake-out physiological saline. The concentration of these resulting suspensions was quantified by standard plate count techniques and defined as 0 h contact time. The remaining vials of each sample were incubated at 37°C for 24 h. After the incubation, the samples contained in the vials were washed out with shake-out physiological saline and plated out as described above, defining the 24 h contact time. All plating was carried out in duplicate. The number of colonies counted was used to calculate the growth values on the control and test samples. The results of this experiment are expressed as mean values of three biological replicates performed.

The antibacterial activity value (A) was calculated using the following formula:

$$A = (lgC_t - lgC_0) - (lgT_t - lgT_0) = F - G \quad (\text{Eq. 4})$$

where

A is the antibacterial activity value;

F is the growth value on the control specimen $F = (lgC_t - lgC_0)$;

G is the growth value on the antibacterial testing specimen $G = (lgT_t - lgT_0)$;

lgC_t is the common logarithm of the arithmetic average of the numbers of bacteria obtained from the control specimen after the 24 h incubation;

lgC_0 is the common logarithm of the arithmetic average of the numbers of bacteria obtained from the control specimen immediately after inoculation;

lgT_t is the common logarithm of arithmetic average of the numbers of bacteria obtained from the antibacterial testing specimens after the 24 h incubation;

lgT_0 is the common logarithm of arithmetic average of the numbers of bacteria obtained from the antibacterial testing specimens immediately after inoculation.

2.5.6 Antimicrobial susceptibility testing by broth microdilution

Antimicrobial susceptibility testing (AST) was performed according to the broth microdilution method of CLSI M07-A10 guidelines [51]. Before performing the evaluation of the activity of both chitosan MWs, a previous MIC test assay was performed to know which concentration of acetic acid could be used to dissolve the chitosan and did not inhibit bacterial growth. Chitosan stock solutions were dispensed in a 96-well round bottom microtiter plate and twofold serially diluted in CAMHB to obtain a concentration range of solutions. A standardized inoculum (2.5.2) was diluted

in CAMHB to ensure that, after inoculation, each well contained approximately 5×10^4 CFU. Each inoculated microtiter plate was incubated under aerobic conditions at 37°C for 24 h. Minimal inhibitory concentration (MIC) values were read as the lowest chitosan concentration for which visible growth was inhibited after 24 h of incubation. For each chitosan stock solution assayed, a growth control (CAMHB and diluted inoculum), a medium sterility control (CAMHB), and a stock solution sterility control (CAMHB and chitosan stock solution) were also tested. The results of this experiment are expressed as median values of three biological replicates performed.

The highest tested concentrations were 0.5 mg/mL and 0.25 mg/mL for LMW and MMW chitosan, respectively. The concentration of acetic acid present at these tested concentrations was lower than the MIC previously determined for this acid.

2.6 Statistical analysis

All data statistically analysed are expressed as means \pm standard errors (SD). Each individual experiment was performed at least in triplicate. The statistical analysis was done using GraphPad Prism 6 (GraphPad Software, Inc., CA). All values were tested for normal distribution and equal variance. When homogeneous variances were confirmed, data were analysed by One Way Analysis of Variance (ANOVA) coupled with the Tukey's post-hoc analysis to identify means with significant differences.

3. Results and Discussion

3.1 Screening and optimization of assays for evaluation of potential wound healing applications of alginate-chitosan aerogel fibres

3.1.1 Aerogel fibres production

To initiate the work, a first batch of fibres was made according to a methodology already established in the laboratory [52]. Some optimizations were made to the process, namely a vacuum aspiration method was developed, replacing the decantation method, to reduce material losses in the step of solvent exchange. This first batch was produced to be further used in the optimization of protocols and assays used to evaluate the potential of these fibres for wound healing applications.

3.1.2 Implementation of sterilization method

Due to the hydrophilicity of the produced fibres, their sterilization by autoclaving with humid heat cannot be done since structural changes, such as fibres contraction or formation of a hydrogel, might occur. One of the most commonly used techniques for sterilization of single-used medical devices is sterilization through radiation, namely ionizing radiation. However, this is a method used by the industry for large-scale productions [53], and not adapted to laboratory scale. Another technique of sterilization by radiation is through UV, a method used in the laboratory for the biological safety cabinet sterilization. This technique, as described by Sabri [44], was adopted for the aerogel fibres sterilization. After the aerogel fibres exposure to UV radiation for 4 h (± 1 h), the sterility test showed no growth of microorganisms, validating the method to ensure the fibres required sterilization. Moreover, in order to evaluate if the sterilization process had no influence on physical or chemical aerogel properties, solid-state characterization was performed before and after UV sterilization. The results obtained showed that the radiation had no influence on the characteristics of the fibres (data not shown).

3.1.3 Implementation of cell culture

The cell line chosen to perform the cell-based assays was the NCTC clone 929 that is described in ISO 10993-5:2009, which is the standard method chosen to evaluate the fibres biocompatibility. After the purchase of the cell line, the culture methods were implemented in the laboratory. Two growth curves were performed using two different seeding densities referenced by the supplier, 10,000 cells/cm² and 30,000 cells/cm², in order to establish the best seeding for the cell culture. The seeding of 30,000 cells/cm² was chosen since it showed more linear growth and allowed the cell subculture twice a week (recommended by the supplier). The seeding of 10,000 cells/cm² showed a slow initial growth which allowed a smaller number of passages per week, and thereby, a smaller number of biological replicates per week (data not shown).

3.1.4 Optimization of cell-based assays

3.1.4.1 Biocompatibility – ISO 10993-5 *in vitro* cytotoxicity assay

Some optimizations were made to the method described in the ISO due to the properties of the fibre material and the concentration defined to carry out the tests. The assay was transferred from 96-well to 24-well plates and optimized, with the same seeding, to provide enough area per well ensuring that the entire sample was in homogeneous contact with the cell monolayer. The cytotoxicity evaluation assay was also modified using the MTS assay, which unlike the MTT method described in ISO, produces a water-soluble formazan [54]. The sample concentration defined for this assay (1.7 mg/mL) was as close as possible to the concentration used in the Dynamic method assay (weighing below 1 mg in the available equipment was not precise).

3.1.4.2 Bioactivity - Scratch assay

Unlike biocompatibility, there is no ISO for the evaluation of cell migration. There are several works of scratch assay with fibroblasts reported in the literature, however, there is still some variability between the described methods [55], [56]. The assay was optimized for 12-well plates using the same cell line and cell seeding of the cytotoxicity assay. After performing the scratch, the plates were incubated with three different times: 8 h, 18 h and 24 h. After 18 h and 24 h periods the scratch was totally closed. After the 8 h incubation, a recovery of about 50% was recorded consistently. The assay was then carried out with the 8 h incubation period, where the scratch only with cells and medium was used as control.

3.1.5 Evaluation of antimicrobial activity: screening and assays optimization

3.1.5.1 Well diffusion and agar plate methods

To evaluate the antimicrobial activity of the fibres, a first screening was performed using the agar plate method and the well diffusion method. There was no evidence of any type of inhibitory halo in both methods (data not shown). The absence of inhibitory halo suggests that the fibres had no antimicrobial activity detectable by the screening methods performed. However, since both methods rely on diffusion of the samples, the absence of halo could mean that the fibres did not diffuse through the agar, making these methods unsuitable for the evaluation of the material produced [57]. Alternatively, two other methods, described below, were selected to evaluate the antimicrobial activity by contact.

3.1.5.2 Static method

Since the intended test material is different that the target material described in ISO 20743:2013 (textile fabrics), some changes and optimizations were made. The method states that the sample mass to be used should be 400 mg. However, compared to the textile fabrics, the aerogels have a very low density, making the fibres extremely light (characteristic of aerogels). As such, the sample mass was reduced to 40 mg and the remaining volumes used in this test were proportionally adapted, keeping the test consistent to what is described.

3.1.5.3 Dynamic method

The ASTM E 2149 – 01 assay was also adopted because it allows to evaluate the antimicrobial activity by varying the time and the contact dynamics of the samples with the bacterial inoculum, when compared with ISO 20743:2013. For this method, the contact time between the samples and the inoculum is suggested to be 1 h or another contact time specified by the researcher. The time required for the fibres (same sample mass used in Static Method 3.1.5.2) to completely dissolve in the working bacterial dilution was tested and was defined as 2.5 h, so that the fibres were in contact with the whole inoculum in a homogeneous way.

In addition to all optimizations, these tests allowed an initial screening, in which a clear antimicrobial activity of the fibres was verified. As such, the evaluation of the antimicrobial activity was a parameter that was determined and that will be discussed in this work.

3.2 Evaluation of alginate-chitosan aerogel fibres for potential wound healing applications

3.2.1 Influence of chitosan molecular weight

One of the objectives of this work was to evaluate the influence of the chitosan MW on the fibre's chemical physical features and potential wound healing properties. In order to understand this influence, fibres were produced varying the chitosan MW, namely fibres with LMW chitosan (alg:chitLMW mass ratio 99:1) and MMW chitosan (alg:chitMMW mass ratio 99:1). These productions were done in duplicate, performing each batch independently.

alg:chitLMW (99:1)



alg:chitMMW (99:1)



Figure 3.1 - Photographs of the aerogel fibres produced with different chitosan MW (low and medium).

The chitosan content (wt.%) of the fibres produced with different chitosan MWs was calculated based on the analysis of nitrogen content. These results, as well as the values for pure chitosans, are shown in Table 3.1. The elemental analysis indicates that both fibres have similar chitosan content (0.7 wt.%). Since the fibres were produced in a ratio of 99:1 (alg:chit), although slightly lower, the obtained result is close to the theoretical value of the fibres chitosan content (1 wt.%). The results of this analysis also indicated that chitosans used in the fibres production were not

totally pure, since they had chitosan contents of 86.3 wt.% and 85.4 wt.% for LMW and MMW, respectively. This may be a reason for the percentages of chitosan content in the aerogels were slightly lower in relation to their theoretical value. Besides the two types of fibres presented similar chitosan contents, also the values between each production batch of both aerogel fibres were similar (data not shown).

Table 3.1 - Chitosan content of alg:chitLMW (99:1) and alg:chitMMW 99:1 aerogel fibres; and respective chitosan raw materials used in their production.

Sample	Nitrogen content (wt.%)	Chitosan content (wt.%)
alg:chitLMW (99:1)	0.06	0.70
alg:chitMMW (99:1)	0.06	0.70
Chitosan (LMW)	7.13	86.3
Chitosan (MMW)	7.06	85.4

Despite being visually equal, that is, both presenting an ultra-light and cotton-like structure, some characterization techniques were applied in order to characterize the aerogel fibres solid-state. To evaluate the morphology of the produced material, SEM micrographs of the fibres produced with the different chitosan MWs were obtained (Figure 3.2). Pictures at higher magnification (30,000x magnification; Figure 3.2b and Figure 3.2d) allowed to verify that produced aerogels are constituted by a network of nanofibers linked to each other, forming porous structures. As in several research works in which the production of aerogels of alginate or chitosan are described [9], [12], these images indicate the efficacy of the scCO₂ drying in preserve the structural integrity of the original hydrogels. Comparing both types of fibres, a similar morphology is observed (Figure 3.2b and Figure 3.2d), indicating that the chitosan MW variation had no influence on the morphology of the produced fibres. SEM micrographs also allowed to verify that between each fibre batch production, morphology of the produced materials was very similar (data not shown).

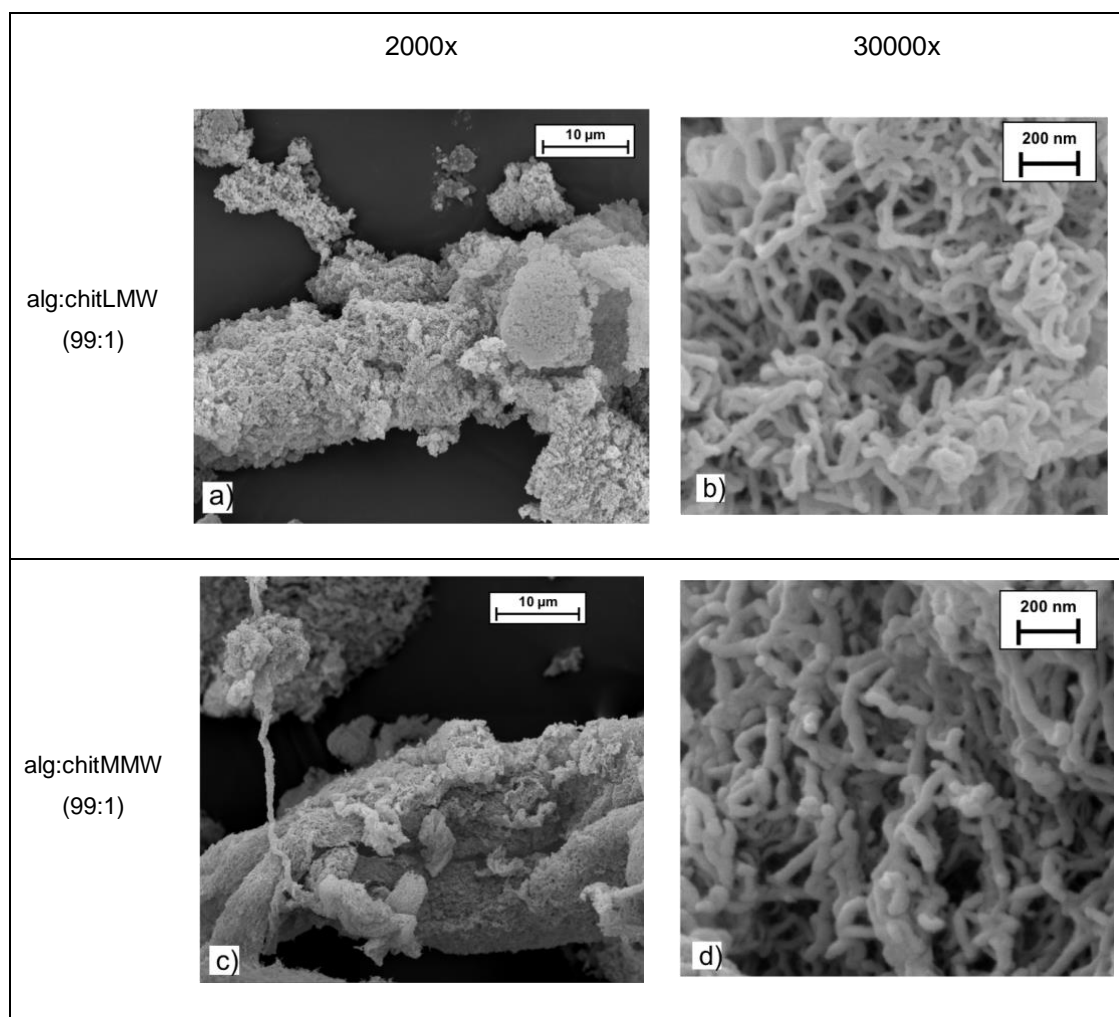


Figure 3.2 - SEM micrographs of alg:chitLMW 99:1 (a,b) and alg:chitMMW 99:1 (c,d) aerogel fibres, at 2000x (a,c) and 30000x (b,d) magnification.

To complement the aerogels solid-state characterization, Figure 3.3 shows the comparison of FTIR spectra of the produced fibres and their pure origin polymers, chitosan (LMW and MMW) and alginate. The typical bands of alginate, corresponding to the two carboxyl groups ($-\text{COOH}$) of the molecular chain, were observed at 1591 cm^{-1} and 1400 cm^{-1} (Figure 3.3a). The FTIR spectrum of LMW (Figure 3.3c) and MMW (Figure 3.3b) chitosan presented, respectively, characteristic peaks of the Amide I at 1645 cm^{-1} and 1647 cm^{-1} and characteristic bands of amino group ($-\text{NH}_2$) at 1572 cm^{-1} and 1566 cm^{-1} . Therefore, spectra of the pure polymers are consistent with those reported in the literature [58]. In the spectra of the fibres produced with LMW and MMW chitosan (Figure 3.3e and Figure 3.3d, respectively), the characteristic peaks of this polymer are not present, whereas the characteristic peaks of alginate are maintained. One of the reasons may be due to the fact that the electrostatic interactions between both polymers have been established in the formation of the hydrogel. However, other explanations may be related to the fact that alginate is at higher mass percentage in the aerogel (99%). Increasing the alginate content, may increase the intensity of its characteristic peaks [59]. This fact associated to the possible overlapping with the characteristic chitosan peaks may justify the obtained results. Although produced with different MW chitosan, spectra of both fibres are quite similar.

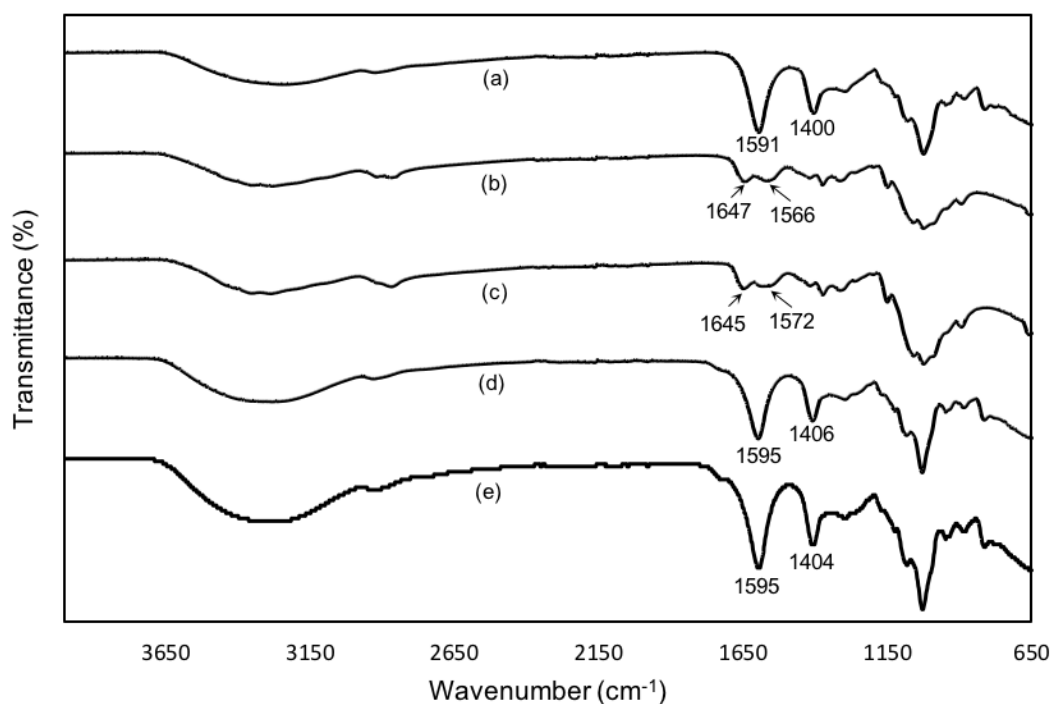


Figure 3.3 - FTIR spectra of (a) sodium alginate, (b) MMW chitosan and (c) LMW chitosan raw materials; (d) alg:chitMMW 99:1 and (e) alg:chitLMW 99:1 aerogel fibres.

In order to evaluate textural properties of the produced aerogels, its surface area and pore volume were characterized (Figure 3.4). In general, these aerogels presented values of surface area (174-261 m²/g) and pore volume (1.41-2.49 cm³/g) within the values of the textural properties of polysaccharide-based aerogels reported in literature [4]. The fibres produced with LMW chitosan showed average surface area values of 257 (±6.36) m²/g and pore volume values of 2.41 (±0.11) cm³/g. On the other hand, the fibres produced with MMW chitosan presented lower average values of surface area, 183 (±12.7) m²/g, and pore volume, 1.81 (±0.56) cm³/g. Therefore, in this analysis, there was a slight difference between the values of the aerogels produced with the different chitosan MWs. One reason that may justify this result is the fact that the MMW chitosan used in the fibres production has a higher viscosity than the LMW. The production of the hydrogel with MMW chitosan may result in a denser PEC limiting the diffusibility of scCO₂. Therefore, higher surface areas and pore volumes may be achieved after supercritical drying of a less dense matrix. These textural properties indicate that the fibres produced with LMW chitosan could achieve higher drug loadings. This is an interesting property that can make these fibres (produced with LMW chitosan) more interesting for wound care applications. Comparing both production batches, similar values were observed between the different productions. These results indicate the reproducibility of the fibre production method in obtaining the aerogel textural properties.

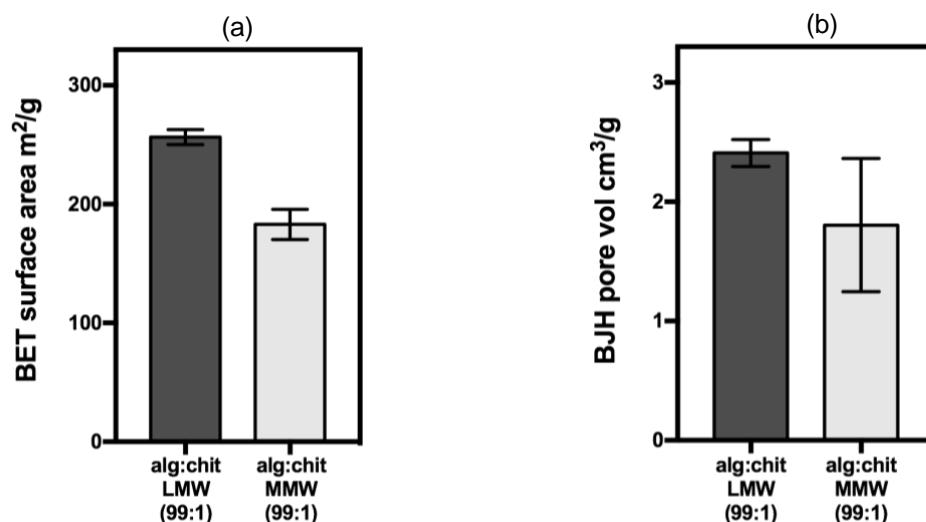


Figure 3.4 - BET surface area (a) and BJH pore volume (b) of alg:chitLMW 99:1 and alg:chitMMW 99:1 aerogel fibres.

Regarding biocompatibility (Figure 3.5), the fibres produced showed no cytotoxicity, since the cell viability value over the control was greater than 70%. This is a result that contributes to the validation of fibres biocompatibility, an important and desired property, since the objective of this work was to evaluate the potential of fibres for an application in direct contact with skin cells. Although the fibres produced in this work are a novel material, the absence of cytotoxicity is a result in accordance with several studies in the literature that have demonstrated the biocompatibility of other types of materials composed of both polymers used in this work. Namely, the work of Kim et al. [60] that demonstrated the absence of cytotoxicity in L929 cells of PEC sponge composed of alginate and chitosan. Also, Shao et al. [61] found that alginate/chitosan hybrid fibre scaffold did not exhibit cytotoxicity in 3T3 fibroblasts. Pure polymers (alginate, LMW and MMW chitosan) used for the fibres production were also evaluated. As shown in Figure 3.5, none of the polymers had percentages of cytotoxicity below 70%, which is in accordance with other studies that have presented alginate and chitosan as biocompatible compounds [23][62]. Moreover, chitosan MW had no influence on pure biopolymer/fibres biocompatibility as demonstrated in the work of Huang et al. [63].

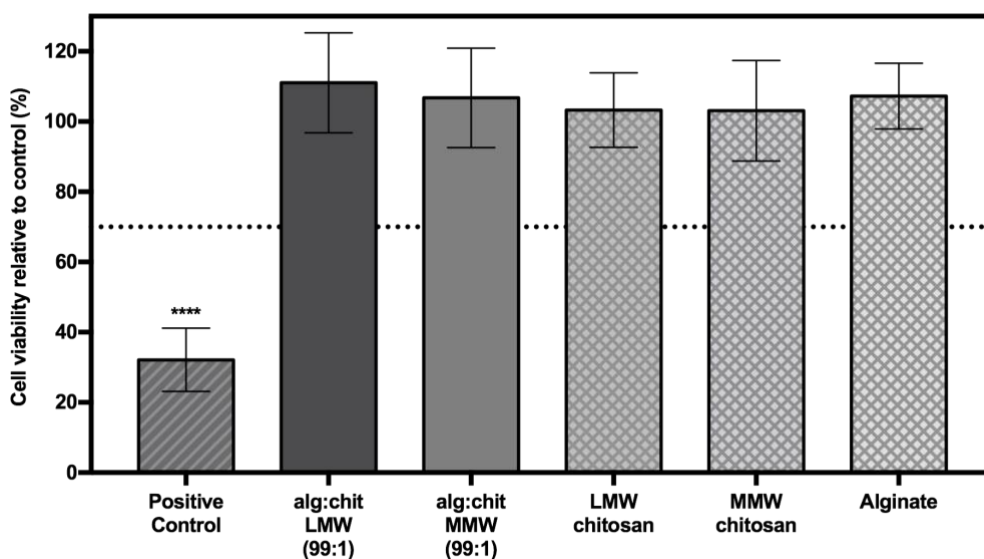


Figure 3.5 - Cytotoxicity assay using MTS reagent: samples (fibres and pure compounds) were incubated, at a concentration of 1.7 mg/mL, in NCTC clone 929 cell line during 24 h at 37°C and 5% CO₂ humidified atmosphere (mean \pm SD, n=3; except controls n=6). Solution of 10% (v/v) of DMSO in cell culture media was used as a positive cytotoxic control. If viability is reduced to <70% of the control, samples have a cytotoxic potential. Statistically significant differences comparing all conditions are indicated by **** ($p < 0.0001$).

After the fibres were found to be non-cytotoxic, the antimicrobial activity of the aerogel fibres was evaluated by the dynamic method. Figure 3.6 shows the percentages of bacterial reduction of *S. aureus* and *K. pneumoniae* when in presence of the different tested samples. Both bacteria, in contact with the produced fibres, presented higher bacterial reduction percentages compared to controls. The statistical analysis showed that there were no statistically significant differences in the bacterial reduction percentages between the different produced fibres as well as between each target bacteria. On the other hand, comparing the bacterial reduction between the two fibres and the controls, a statistical different behaviour was observed. Since the antimicrobial activity in this method is measured in terms of bacterial reduction, these results indicate that these aerogel fibres showed clear antimicrobial activity against bacteria representative of wound infectious microbiota. Other studies, where the antimicrobial activity was evaluated using the same standard method (ASTM E 2149), also demonstrated antimicrobial activity of similar materials produced with these same polymers [64], [65]. However, the fact that there were no statistically significant differences indicates that the MW variation in the fibres production had no influence on their antimicrobial activity, for the conditions tested.

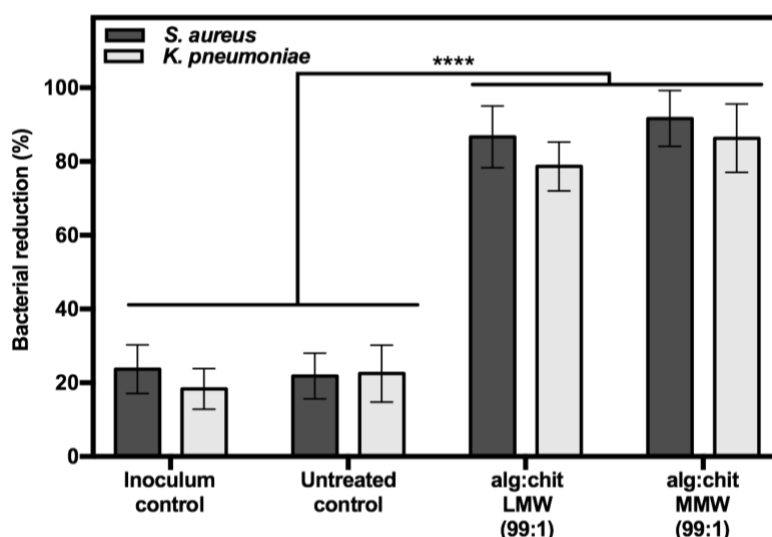


Figure 3.6 - Percent reduction of *S. aureus* and *K. pneumoniae* resulting from contact with samples, at a concentration of 0.8 mg/mL, during 2.5 h at 37°C (mean \pm SD, n=3; except controls n=6). Cotton disks were used as untreated control. Statistically significant differences observed between all fibre conditions are indicated by **** (p < 0,0001).

Table 3.2 shows the values of the antimicrobial activity and its effectiveness calculated by the static method. In this method, which allows to categorize the activity of the tested materials as significant ($2 \leq$ antibacterial value < 3) or strong (antibacterial value ≥ 3), all the fibres showed strong efficacy against both bacteria. Therefore, as in the previous method, these results indicate a clear antimicrobial activity of the produced fibres. Comparing this antimicrobial activity, both fibres presented again very similar values as in the previous method (Figure 3.6). There was a slightly superior antibacterial activity of the fibres produced with LMW chitosan against *S. aureus*, whereas the fibres produced with MMW chitosan presented a slightly superior activity for *K. pneumoniae*.

Table 3.2 - Antimicrobial property efficacy of the tested material against *S. aureus* and *K. pneumoniae* from contact with samples, at a concentration of 2 g/mL, during 24 h at 37°C (mean \pm SD, n=3). Efficacy is defined as significant (for $2 \leq$ antibacterial value < 3), strong (for antibacterial value ≥ 3), or N/A (not applicable for values < 2).

Strain	Aerogel Fibre (w/w)	Antibacterial value	Efficacy
<i>S. aureus</i>	alg:chitLMW (99:1)	5.8	Strong
	alg:chitMMW (99:1)	5.2	Strong
<i>K. pneumoniae</i>	alg:chitLMW (99:1)	5.4	Strong
	alg:chitMMW (99:1)	5.7	Strong

In order to understand if the molecular weight of the chitosan used in the fibres production influenced the antimicrobial activity of this polymer, the MIC of both molecular weights against the chosen target bacteria was tested. The concentration of acetic acid used to dissolve both chitosans, measured by AST, that did not inhibit bacterial growth was 0.02% (v/v). After contact

of the polymers with the bacteria the MIC values (Table 3.3) of LMW chitosan were 0.50 mg/mL and 0.25 mg/mL for *S. aureus* and *K. pneumoniae*, respectively. For MMW chitosan both bacteria had a MIC of 0.25 mg/mL. The determined MIC values were almost similar for both MWs and both bacteria, showing that MW variation does not greatly impact the antimicrobial activity of the tested chitosans. Although for *S. aureus* a difference of twice the MIC between LMW and MMW could be observed, according to the standard method used [51], this difference is not considered significant to conclude that there is a clear differences between the antimicrobial activities of the two MWs. Although the literature is still somewhat contradictory on the influence of MW [27], [66], the results obtained in this work are in agreement with the work done by No et al. [26], which also recorded very little significant differences in the MICs between chitosan MWs against a wide range of microorganisms. Also, the tested chitosans did not have a specific MW value but a range of MW values, from 50-190 kDa (LMW) and 190-310 kDa (MMW). In addition, the MW difference between both ranges is not very significant when compared to chitosan MWs tested in the literature.

Table 3.3 – Antimicrobial susceptibility testing of low and medium MW chitosans against *S. aureus* and *K. pneumoniae*. Median and triplicate values of MICs (mg/mL) are presented.

Bacteria	MIC (mg/mL)	
	LMW Chitosan	MMW Chitosan
<i>S. aureus</i>	0.50 (0.25/0.50/0.50)	0.25 (0.25/0.25/0.25)
<i>K. pneumoniae</i>	0.25 (0.25/0.25/0.25)	0.25 (0.25/0.25/0.25)

The LMW chitosan compared to MMW has much lower viscosity, allowing more concentrated solutions and being more convenient to work with. In addition, the fibres produced with this chitosan presented surface area and pore volume values higher than the aerogels produced with MMW chitosan. The increase of surface area and pore volume of the aerogels may allow greater drug loadings [67]. This is an interesting factor, since for wound healing applications, these fibres produced with LMW chitosan may achieve higher loading of bioactive compounds that also contribute to the acceleration of the wound healing process. Therefore, the LMW was chosen and used for the following tests of this work.

3.2.2 Influence of chitosan content

Another objective of this work was to evaluate the influence of chitosan content on the final characteristics of aerogel fibres. Therefore, aerogel fibres were produced by varying the content of LMW chitosan added in the Sol-Gel process step. In addition to the already produced fibres with a mass ratio of 99:1 between alginate and LMW chitosan, new aerogel fibres were obtained with mass ratios between both polymers of 19:1 and 9:1. These productions were done in duplicate, performing each batch independently.



Figure 3.7 - Photographs of the aerogel fibres produced with different chitosan content.

Regarding the solid-state characterization, Table 3.4 shows the values of the chitosan content of each aerogel fibre. Given the mass ratios between alginate and chitosan, 99:1, 19:1 and 9:1, the theoretical values of the chitosan content of each fibre would be 1 wt.%, 5 wt.% and 10 wt.%, respectively. Aerogel fibres presented chitosan content values close to their theoretical values. However, the chitosan content of the alg:chitLMW 19:1 and alg:chitLMW 9:1 aerogel fibres presented higher values than the theoretical chitosan content. Between the different production batches each type of fibre showed similar values of chitosan content (data not shown).

Table 3.4 - Chitosan content of alg:chitLMW 99:1, 19:1 and 9:1 aerogel fibres; and respective chitosan raw material used in their production.

Sample	Nitrogen content (wt.%)	Chitosan content (wt.%)
alg:chitLMW (99:1)	0.06	0.70
alg:chitLMW (19:1)	0.46	5.40
alg:chitLMW (9:1)	0.98	11.9
Chitosan (LMW)	7.13	86.3

Figure 3.8 shows the SEM micrographs of the fibres produced with the different polymer proportions. Comparing the images of the three fibres with different chitosan contents, this variation did not register outstanding morphological differences in the produced fibres. In the pictures at higher magnification, Figure 3.8b, d and f show a similar texture of a nanofibers network linked to each other, forming highly porous structures. In addition, the same fibres obtained in different production batches presented very similar morphologies, thus demonstrating the reproducibility of the production process (data not shown).

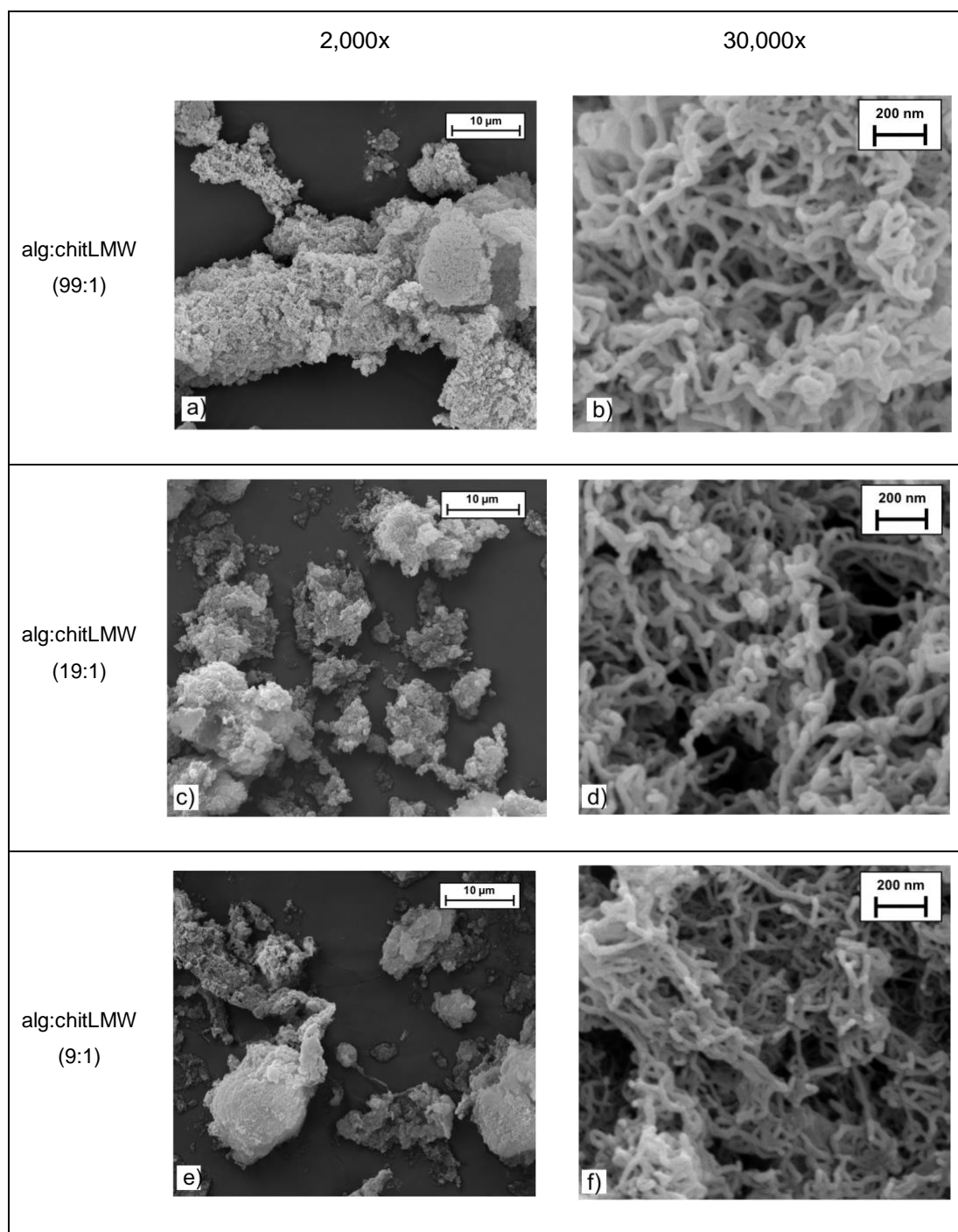


Figure 3.8 - SEM micrographs of alg:chitLMW 99:1 (a,b), alg:chitLMW 19:1 (c,d) and alg:chitLMW 9:1 (e,f) aerogel fibres, at 2,000x (a,c,e) and 30,000x (b,d,f) magnification.

Regarding fibres chemical composition, Figure 3.9 shows the comparison of FTIR spectra of the aerogel fibres produced with different LMW chitosan contents and their pure origin polymers, LMW chitosan and alginate. Aerogel fibres presented a spectrum quite similar to the one of pure alginate. However, comparing the spectra of the different fibres, there is a reduction in the transmittance of the characteristic peaks of the alginate (1595 cm^{-1} , 1408 cm^{-1}), as the fibres chitosan content increases. With this increase, a peak (1713 cm^{-1}) appears in the fibres with higher chitosan content (Figure 3.9c) possibly corresponding to a shifted characteristic peak of the chitosan Amide I (1645 cm^{-1}). This result indicates a slight difference between the different

fibres spectra, possibly related to the mass ratio variation of alginate and chitosan in the fibres production. On the other hand, the peak corresponding to the chitosan amine group (1572 cm^{-1}) disappears in all aerogels' spectra, as already observed and discussed in the previous section (3.2.1; Figure 3.3). FTIR spectra of the fibres produced in different batches were practically identical, indicating reproducibility of the production process (data not shown).

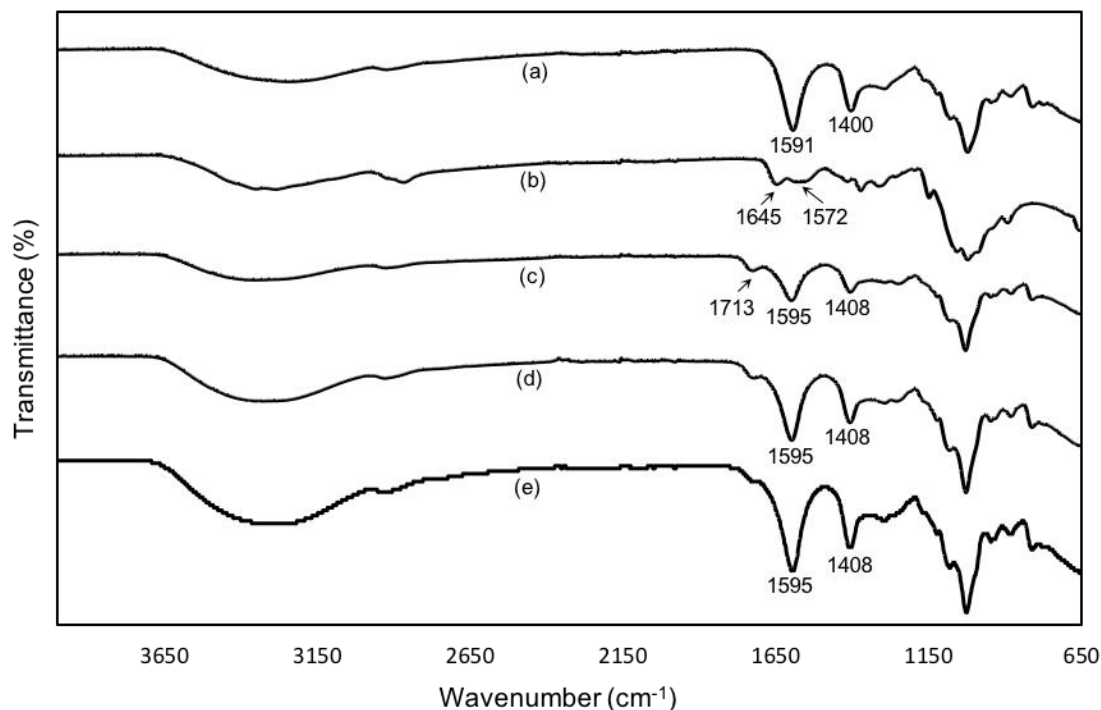


Figure 3.9 - FTIR spectra of (a) sodium alginate and (b) LMW chitosan raw materials; (c) alg:chitLMW 9:1, (d) alg:chitLMW 19:1 and (e) alg:chitLMW 99:1 aerogel fibres.

Surface area (Figure 3.10a) and pore volume (Figure 3.10b) values of the aerogel fibres produced with the different chitosan contents are presented in Figure 3.10. In general, like for the aerogels discussed in the previous section (3.2.1; Figure 3.4), these aerogels presented values of surface area ($179\text{-}302\text{ m}^2/\text{g}$) and pore volume ($1.59\text{-}2.49\text{ cm}^3/\text{g}$) within the values of the textural properties of polysaccharide-based aerogels reported in literature [4]. Comparing the mean values of both analyses for the different types of fibres, slight differences between them are observed. The fibres with the polymer ratio of 99:1, 19:1 and 9:1 showed mean surface area values of $257 (\pm 6.40)\text{ m}^2/\text{g}$, $250 (\pm 73.5)\text{ m}^2/\text{g}$ and $171 (\pm 12.0)\text{ m}^2/\text{g}$, respectively. On the other hand, the mean pore volume values for these fibres were respectively $2.41 (\pm 0.11)\text{ cm}^3/\text{g}$, $2.08 (\pm 0.35)\text{ cm}^3/\text{g}$ and $1.68 (\pm 0.12)\text{ cm}^3/\text{g}$. These results indicate a decrease in the mean values of surface area and pore volume with increasing chitosan content in the fibres. Increasing the chitosan content increases the ratio of both polymers, promoting the establishment of more polyanion-polycation interactions, resulting in the formation of more complex aggregates, and a denser PEC [68]. As mentioned in the previous section (3.2.1), a denser hydrogels matrix may lead to lower surface areas and pore volumes of resulting aerogels. Comparing both production

batches, similar values were observed between the different productions with the exception of the alg:chitLMW 19:1 aerogel fibres, which presented the highest standard deviation and high error percentage of surface area and pore volume. One reason that may justify this discrepancy was the fact that there was a considerable loss of hydrogel mass during the solvent exchange of the second batch of these fibres. Thus, in the supercritical drying step, the filter paper containing the hydrogel had much lower mass. The first batch fibres presented surface area and pore volume values of 198 m²/g and 1.83 cm³/g, respectively. On the other hand, the fibres of the second production batch, presented higher values for the same properties, with 302 m²/g and 2.33 cm³/g, respectively. As such, the drying process of discrepant hydrogel masses may have led to discrepant textural properties, between the different batches.

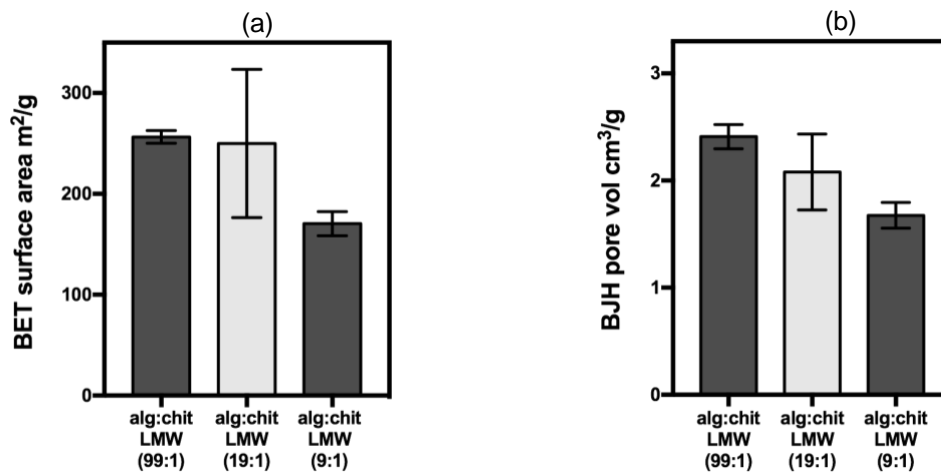


Figure 3.10 - BET surface area (a) and BJH pore volume (b) of alg:chitLMW 99:1, 19:1 and 9:1 aerogel fibres.

In the following cellular and antimicrobial assays, the results of a commercial medical device chosen in order to compare with the material produced in this work are also presented. The chosen material was a sterile calcium sodium alginate dressing, indicated for moderately to highly exuding chronic and acute wounds - Kaltostat®.

Figure 3.11 shows the cell viability values obtained after the contact of the cells with the aerogel fibres produced with different chitosan contents and the commercial medical device. All fibres, as well as Kaltostat®, presented cell viability values over the control greater than 70%. As such, this result indicates that none of the fibres nor the medical device were cytotoxic in the tested conditions, demonstrating the aerogel fibres' suitability for applications in contact with skin cells.

Like the MW, also the fibres' chitosan content had no influence on cell viability in the tested conditions.

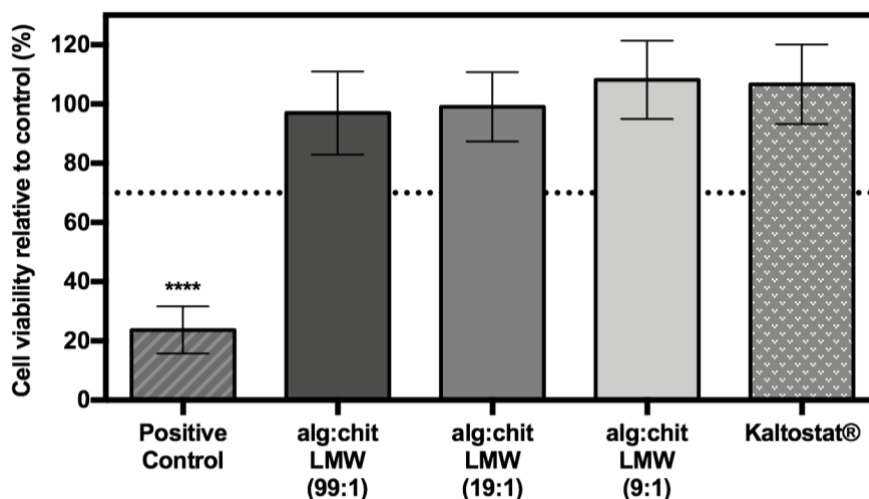


Figure 3.11 - Cytotoxicity assay using MTS reagent: samples were incubated, at a concentration of 1.7 mg/mL, in NCTC clone 929 cell line during 24 h at 37°C and 5% CO₂ humidified atmosphere (mean \pm SD, n=3; except controls n=6). Solution of 10% (v/v) of DMSO in cell culture media was used as a positive cytotoxic control. If viability is reduced to <70% of the control, samples have a cytotoxic potential. Statistically significant differences comparing all conditions are indicated by **** (p < 0,0001).

Since aerogel fibres were found to be non-cytotoxic, their ability to stimulate wound closure on an *in vitro* scale was assessed (Figure 3.12). Aerogel fibres and Kaltostat® presented percentages of recovered area about 75%, higher than untreated control (~50%). This difference was statistically significant, indicating that the produced fibres have the ability to stimulate migration of skin cells involved in the wound healing process. Also, in the literature, the ability of materials composed by these two polymers to accelerate wound healing in *in vivo* rat models has been verified [69], [70]. As shown from the statistical analysis, differences between the different fibres and Kaltostat® were not statistically significant. The fact for not being able to register significant differences between the different tested materials may be due to several factors. The high cellular proliferation of the used cell line, the short period of samples contact time (8 h) and the scratch small area. It was possible to verify the fibres bioactivity but no statistically significant differences between them.

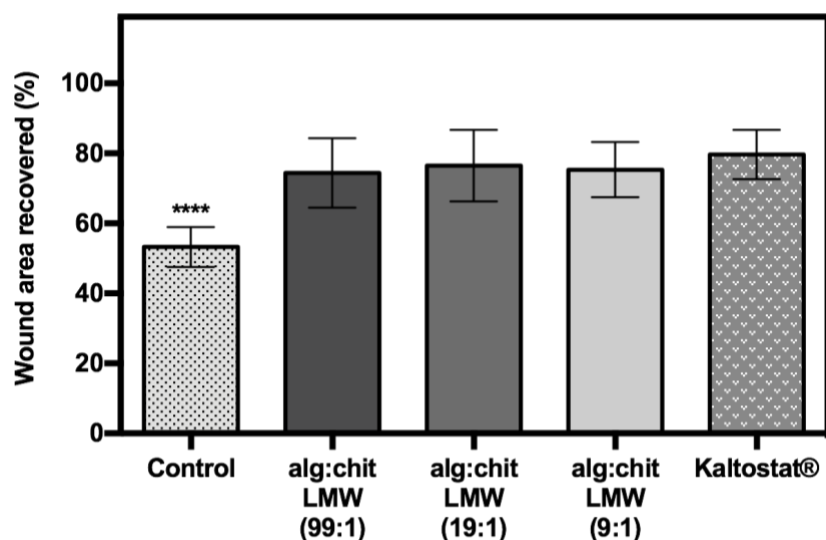


Figure 3.12 - Scratch assay: samples were incubated, at a concentration of 1.7 mg/mL, in NCTC clone 929 fibroblasts, during 8h at 37°C and 5% CO₂ humidified atmosphere (mean \pm SD, n=4). Statistically significant differences when compared to control conditions are indicated by **** (p < 0.0001).

Regarding the antibacterial activity, Figure 3.13 and Figure 3.14 show the percentages of bacterial reduction, measured by the dynamic method, of *S. aureus* and *K. pneumoniae*, respectively, when in presence of the different tested samples. Both bacteria, in contact with all produced fibres, presented higher percentages reduction compared to controls as well as with Kaltostat®. *S. aureus* (Figure 3.13) showed a slight decrease tendency of the percentage reduction as the fibre's chitosan content increases. In contrast, *K. pneumoniae* (Figure 3.14) presented a tendency of this percentage to increase. However, there were no statistically significant differences between the different fibres for each target bacteria. This indicates that the variation of chitosan content in the fibres had no clear influence on the percentage reduction for each target bacteria. On the other hand, the statistical analysis showed that the difference between fibres and the remaining conditions (inoculum only control, untreated control and Kaltostat®) was statistically significant, indicating a clear antimicrobial activity of the aerogel fibres.

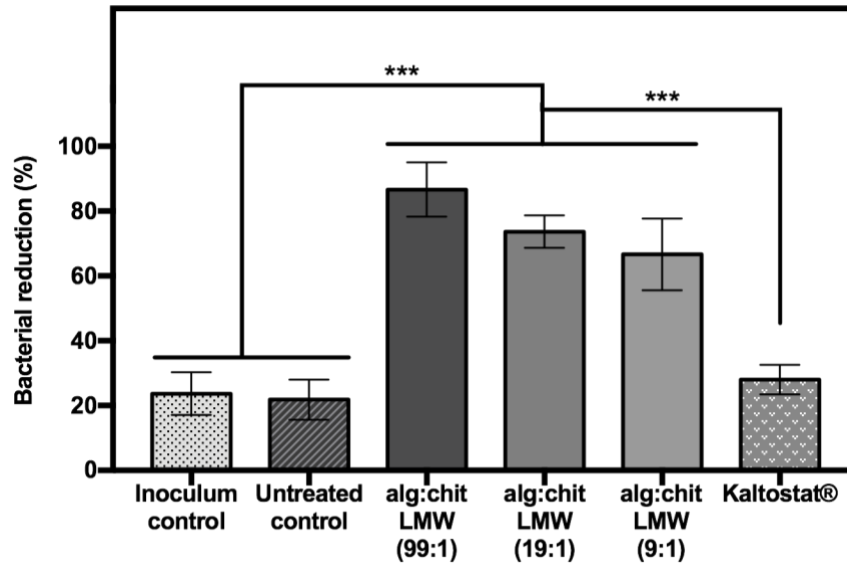


Figure 3.13 - Percent reduction of *S. aureus* resulting from contact with samples, at a concentration of 0.8 mg/mL, during 2.5 h at 37°C (mean \pm SD, n=3; except controls n=6). Cotton disks were used as untreated control. Statistically significant differences observed between all conditions are indicated by *** (at least $p \leq 0.0004$).

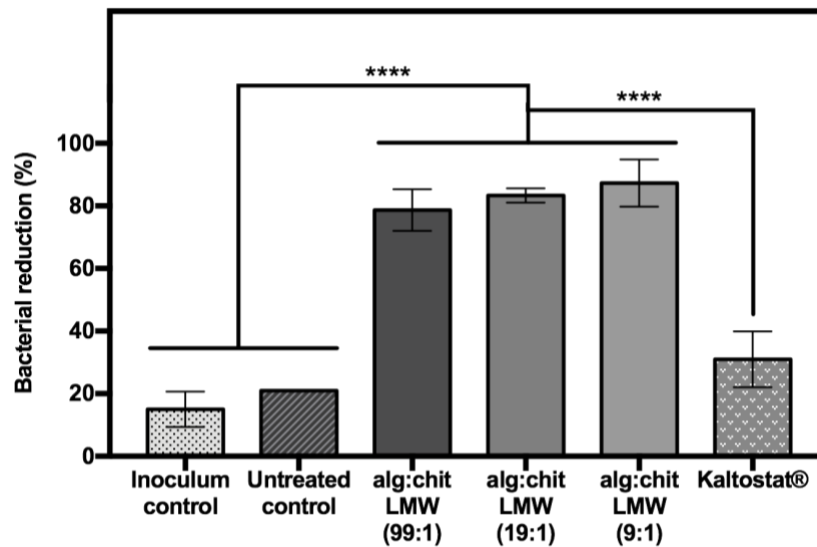


Figure 3.14 - Percent reduction of *K. pneumoniae* resulting from contact with samples, at a concentration of 0.8 mg/mL, during 2.5 h at 37°C (mean \pm SD, n=3; except controls n=6). Cotton disks were used as untreated control. Statistically significant differences observed between all conditions are indicated by **** ($p < 0.0001$).

In Figure 3.15, all the conditions between each target bacteria, in the presence of the different samples, were compared and an inverse tendency of the bacterial activity of the fibres for both microorganisms was again demonstrated. However, there were only statistically significant differences between both bacteria for the fibres with the highest chitosan content (alg:chitLMW 9:1). One reason that may explain this difference in activity between the tested bacteria is that chitosan can, in part, exert a specific and differential antimicrobial activity between gram-positive

and gram-negative bacteria [27]. Also, fibres with higher chitosan content were found to take longer to dissolve in the working bacterial dilution. As such, altering the polymers mass ratio on the fibres production, can alter some fibres properties such as the bioavailability of elements that exert the fibres antimicrobial activity. In addition, the fact that the antimicrobial activity was assessed only for a single short contact time does not allow the perception of the activity variation over time.

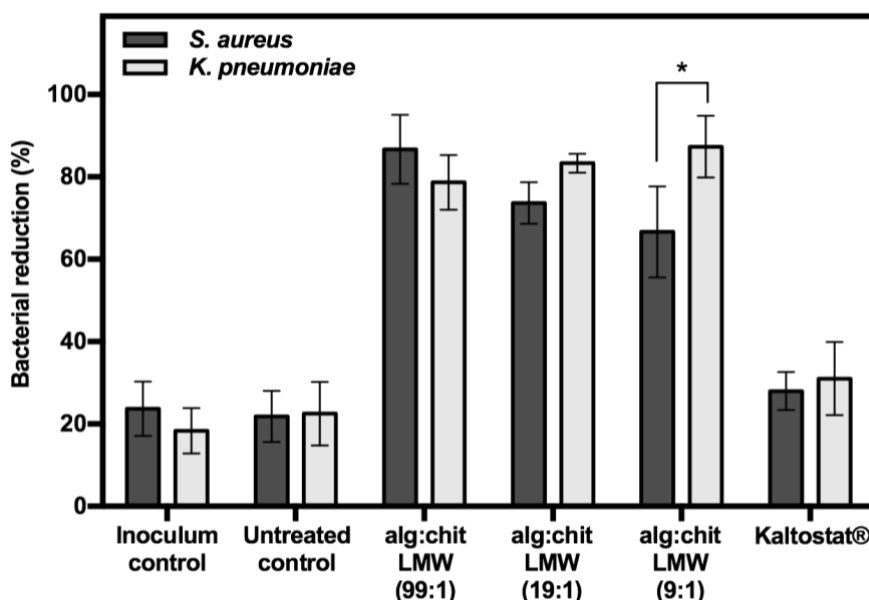


Figure 3.15 - Percent reduction of *S. aureus* and *K. pneumoniae* resulting from contact with samples, at a concentration of 0.8 mg/mL, during 2.5 h at 37°C (mean \pm SD, n=3; except controls n=6). Cotton disks were used as untreated control. Statistically significant differences observed between all fibre conditions are indicated by * ($p < 0.05$).

The values presented in Table 3.5 demonstrate the efficacy of the antimicrobial activity comparing the different fibres and Kaltostat®, by the static method. The obtained results show that all fibres presented strong efficacy against both bacteria. Comparatively, Kaltostat® showed less activity, with efficacy characterized as significant against *K. pneumoniae* whereas for *S. aureus* the activity value was not enough to be considered effective. Therefore, as in the previous method, these results indicate a clear antimicrobial activity of the produced fibres, even comparing with (Kaltostat®).

This method showed a tendency of the antimicrobial activity to increase with the increase of the fibre's chitosan content for both bacteria. These results therefore showed a fibres behaviour slightly different from the results obtained by the contact method (Figure 3.15). However, the methodologies are quite different and as such the comparison of the results between both methods should not be done directly.

Considering only the chitosan concentration factor, it is known that an increase in its concentration increases the number of amine groups available for the occurrence of electrostatic interactions with anionic components of microorganisms [27]. As such, considering only this factor, there may be a proportional relationship between fibres activity and chitosan content. However, not only free

chitosan was tested, but a PEC. This assumes that some of the amine groups of chitosan were involved in electrostatic interactions with alginate. As such, another factor to be studied is whether, due to the interactions between both polymers, the increasing of chitosan content may or may not signify a proportional increase of the free amine groups to interact with the microorganisms. In order to verify whether the increase of the antimicrobial activity recorded in this assay is in fact related to the increase of fibres chitosan content.

Table 3.5 - Efficacy of antibacterial property of the tested material against *S. aureus* and *K. pneumoniae* from contact with samples, at a concentration of 2 g/mL, during 24 h at 37°C (mean \pm SD, n=3). Efficacy is defined as significant ($2 \leq$ antibacterial value < 3), strong (antibacterial value ≥ 3), and N/A (not applicable for values < 2).

Strain	Sample (w/w)	Antibacterial value	Efficacy
<i>S. aureus</i>	alg:chitLMW (99:1)	5.8	Strong
	alg:chitLMW (19:1)	5.5	Strong
	algi:chitLMW (9:1)	6.6	Strong
	Kaltostat®	1.6	N/A
<i>K. pneumoniae</i>	alg:chitLMW (99:1)	5.4	Strong
	alg:chitLMW (19:1)	6.2	Strong
	algi:chitLMW (9:1)	7.1	Strong
	Kaltostat®	2.1	Significant

4. Conclusion

In the present thesis the potential wound healing applications of alginate-chitosan aerogel fibres was investigated. Even though there are several studies reporting the suitability for tissue regeneration applications of various materials produced with these two marine polymers (alone or in combination), this is the first demonstration of the production of alginate-chitosan aerogel fibres and its solid-state, biocompatibility and bioactivity characterization.

The organic aerogel fibres were prepared by three step procedure, which involves the formation of a hydrogel between both polymers through the sol-gel process, solvent exchange and supercritical drying. The textural analysis by SEM and nitrogen adsorption revealed that the produced aerogels are a network of nanofibers linked to each other, forming highly porous structures with high specific surface area and pore volume values. The chemical characterization through FTIR and the chitosan content through elemental analysis allowed to verify the presence of both polymers and the content of chitosan close to its theoretical percentage. Regarding biocompatibility and cellular bioactivity, the mouse fibroblasts NCTC clone 929 cell line used for the *in vitro* assays was successfully implemented in the laboratory. The cell-based assays revealed that produced aerogels are non-cytotoxic and bioactive, accelerating the wound closure of an *in vitro* scale model. The standard tests chosen to evaluate the antimicrobial activity allowed this characterization with success, adapting to the physical and chemical properties of the produced fibres. These results allowed to verify a clear antimicrobial activity of the fibres using two distinct methodologies with different contact times and dynamics of the samples with the chosen bacteria inoculums.

The chitosan MW and content were varied during aerogel productions in order to evaluate the influence of these factors on the analysed characteristics of the fibres. The MWs of chitosan influenced the aerogel's textural properties, slightly decreasing their specific surface area and pore volume with increasing MW. Also, the chitosan content, and consequently the mass ratio variation between both polymers, influenced the fibre's specific surface area and pore volume, with a decrease of these values with the decrease of the ratio between alginate and chitosan (increasing the fibre's chitosan content). Regarding the remaining performed characterizations, these two factors did not present significant differences that justified a clear influence on the fibre's properties.

In addition, after comparison with a commercial medical device (Kaltostat®) for wound healing applications, the fibres were found to have a similar cellular behaviour, and a clearly superior antimicrobial activity. The obtained results suggest that these alginate-chitosan aerogel fibres are good candidates for wound healing applications. This potential of the produced material opens the perspective for future works. Namely, a more detailed characterization of this material in order to confer greater robustness to the aerogel fibres potential. Other important properties for wound healing applications such as water uptake, mechanical strength and non-allergic reactions should therefore be characterized. The future work should also focus on a variation of chitosan MWs and polymer mass ratios very different from those tested, in order to verify the influence of these

factors. Regarding the biocompatibility and cell migration assays, the use of other skin cells (e.g. keratinocytes), coculture models or mouse assays, in an *in vivo* perspective will also be interesting aspects to investigate in the future. In addition, studying the impregnation of drugs or bioactive compounds, exploring the high porosity of aerogel, will also be interesting. These compounds may confer new or improved physical and biological properties to aerogel fibres. Finally, the study of incorporation of chitosan recovery from food industry waste into the overall fibres production process would be also interesting, contributing to a more sustainable production process.

A submitted abstract of this work was selected for an oral presentation at the 13th International Chemical and Biological Engineering Conference (CHEMPOR 2018) held in Aveiro - Portugal, from the 2nd to the 4th of October, 2018.

5. References

- [1] J. Stergar and U. Maver, "Review of aerogel-based materials in biomedical applications," *J. Sol-Gel Sci. Technol.*, vol. 77, no. 3, pp. 738–752, 2016.
- [2] R. Subrahmanyam, P. Gurikov, P. Dieringer, M. Sun, and I. Smirnova, "On the Road to Biopolymer Aerogels—Dealing with the Solvent," *Gels*, vol. 1, no. 2, pp. 291–313, 2015.
- [3] H. Maleki, L. Durães, C. A. García-González, P. del Gaudio, A. Portugal, and M. Mahmoudi, "Synthesis and biomedical applications of aerogels: Possibilities and challenges," *Adv. Colloid Interface Sci.*, vol. 236, 2016.
- [4] C. A. García-González, M. Alnaief, and I. Smirnova, "Polysaccharide-based aerogels - Promising biodegradable carriers for drug delivery systems," *Carbohydr. Polym.*, vol. 86, no. 4, pp. 1425–1438, 2011.
- [5] E. Elizondo, J. Veciana, and N. Ventosa, "Nanostructuring molecular materials as particles and vesicles for drug delivery, using compressed and supercritical fluids," *Nanomedicine*, vol. 7, no. 9, pp. 1391–1408, Sep. 2012.
- [6] B. Subramaniam, R. A. Rajewski, and K. Snavely, "Pharmaceutical processing with supercritical carbon dioxide," *J. Pharm. Sci.*, vol. 86, no. 8, pp. 885–890, 1997.
- [7] R. Subrahmanyam, P. Gurikov, I. Meissner, and I. Smirnova, "Preparation of Biopolymer Aerogels Using Green Solvents," *J. Vis. Exp.*, vol. 2, no. 113, pp. 3–7, 2016.
- [8] P. Yadav, H. Yadav, V. G. Shah, G. Shah, and G. Dhaka, "Biomedical biopolymers, their origin and evolution in biomedical sciences: A systematic review," *J. Clin. Diagnostic Res.*, vol. 9, no. 9, pp. 21–25, 2015.
- [9] M. Robitzer, L. David, C. Rochas, F. Di Renzo, and F. Quignard, "Nanostructure of calcium alginate aerogels obtained from multistep solvent exchange route," *Langmuir*, vol. 24, no. 21, pp. 12547–12552, 2008.
- [10] M. Martins *et al.*, "Preparation of macroporous alginate-based aerogels for biomedical applications," *J. Supercrit. Fluids*, vol. 106, 2015.
- [11] M. R. Ayers and A. J. Hunt, "Synthesis and properties of chitosan-silica hybrid aerogels," *J. Non. Cryst. Solids*, vol. 285, no. 1–3, pp. 123–127, 2001.
- [12] F. Quignard, R. Valentin, and F. Di Renzo, "Aerogel materials from marine polysaccharides," *New J. Chem.*, vol. 32, no. 8, pp. 1300–1310, 2008.
- [13] K. Y. Lee and D. J. Mooney, "Alginate: Properties and biomedical applications," *Prog. Polym. Sci.*, vol. 37, no. 1, pp. 106–126, 2012.
- [14] K. I. Draget, "Alginates," *Handb. Hydrocoll. Second Ed.*, pp. 807–828, 2009.
- [15] S. N. Pawar and K. J. Edgar, "Alginate derivatization: A review of chemistry, properties and applications," *Biomaterials*, vol. 33, no. 11, pp. 3279–3305, 2012.
- [16] I. D. Hay, Y. Wang, M. F. Moradali, Z. U. Rehman, and B. H. A. Rehm, "Genetics and regulation of bacterial alginate production," *Environ. Microbiol.*, vol. 16, no. 10, pp. 2997–3011, 2014.
- [17] M. George and T. E. Abraham, "Polyionic hydrocolloids for the intestinal delivery of protein drugs: Alginate and chitosan - a review," *J. Control. Release*, vol. 114, no. 1, pp. 1–14, 2006.
- [18] J. Sun and H. Tan, "Alginate-based biomaterials for regenerative medicine applications," *Materials (Basel)*, vol. 6, no. 4, pp. 1285–1309, 2013.
- [19] V. Zargar, M. Asghari, and A. Dashti, "A Review on Chitin and Chitosan Polymers: Structure, Chemistry, Solubility, Derivatives, and Applications," *ChemBioEng Rev.*, vol. 2, no. 3, pp. 204–226, 2015.
- [20] M. Rinaudo, "Chitin and chitosan: Properties and applications," *Prog. Polym. Sci.*, vol. 31, no. 7, pp. 603–632, 2006.
- [21] M. N. . Ravi Kumar, "A review of chitin and chitosan applications," *React. Funct. Polym.*,

- vol. 46, no. 1, pp. 1–27, 2000.
- [22] E. Khor and A. C. A. Wan, *Chitin: Fulfilling a Biomaterials Promise: Second Edition*. 2014.
 - [23] A. Tiwari and A. N. Nordin, *Advanced Biomaterials and Biodevices*. 2014.
 - [24] W. Paul and C. Sharma, "Chitosan and alginate wound dressings: a short review," *Trends Biomater Artif Organs*, vol. 18, no. 1, pp. 18–23, 2004.
 - [25] R. Jayakumar, D. Menon, K. Manzoor, S. V. Nair, and H. Tamura, "Biomedical applications of chitin and chitosan based nanomaterials - A short review," *Carbohydr. Polym.*, vol. 82, no. 2, pp. 227–232, 2010.
 - [26] H. K. No, N. Young Park, S. Ho Lee, and S. P. Meyers, "Antibacterial activity of chitosans and chitosan oligomers with different molecular weights," *Int. J. Food Microbiol.*, vol. 74, no. 1–2, pp. 65–72, 2002.
 - [27] M. Kong, X. G. Chen, K. Xing, and H. J. Park, "Antimicrobial properties of chitosan and mode of action: A state of the art review," *Int. J. Food Microbiol.*, vol. 144, no. 1, pp. 51–63, 2010.
 - [28] V. S. Meka, M. K. G. Sing, M. R. Pichika, S. R. Nali, V. R. M. Kolapalli, and P. Kesharwani, "A comprehensive review on polyelectrolyte complexes," *Drug Discov. Today*, vol. 22, no. 11, pp. 1697–1706, 2017.
 - [29] Y. Luo and Q. Wang, "Recent development of chitosan-based polyelectrolyte complexes with natural polysaccharides for drug delivery," *Int. J. Biol. Macromol.*, vol. 64, pp. 353–367, 2014.
 - [30] A. M. Alsharabasy, S. A. Moghannem, and W. N. El-Mazny, "Physical preparation of alginate/chitosan polyelectrolyte complexes for biomedical applications," *J. Biomater. Appl.*, vol. 30, no. 7, pp. 1071–1079, 2016.
 - [31] C. Schatz, J. M. Lucas, C. Viton, A. Domard, C. Pichot, and T. Delair, "Formation and properties of positively charged colloids based on polyelectrolyte complexes of biopolymers," *Langmuir*, vol. 20, no. 18, pp. 7766–7778, 2004.
 - [32] I. C. Liao, A. C. A. Wan, E. K. F. Yim, and K. W. Leong, "Controlled release from fibers of polyelectrolyte complexes," *J. Control. Release*, vol. 104, no. 2, pp. 347–358, 2005.
 - [33] G. Han and R. Ceilley, "Chronic Wound Healing: A Review of Current Management and Treatments," *Adv. Ther.*, vol. 34, no. 3, pp. 599–610, 2017.
 - [34] A. C. de O. Gonzalez, T. F. Costa, Z. de A. Andrade, and A. R. A. P. Medrado, "Wound healing - A literature review," *An. Bras. Dermatol.*, vol. 91, no. 5, pp. 614–620, 2016.
 - [35] R. F. Diegelmann, "Wound healing: an overview of acute, fibrotic and delayed healing," *Front. Biosci.*, vol. 9, no. 1–3, p. 283, 2004.
 - [36] J. Percival, Nicholas, "Classification of wounds and their treatment," *Surgery*, vol. 20, no. 5, pp. 114–117, 2002.
 - [37] J. Boateng and O. Catanzano, "Advanced Therapeutic Dressings for Effective Wound Healing - A Review," *J. Pharm. Sci.*, vol. 104, no. 11, pp. 3653–3680, 2015.
 - [38] R. Edwards and K. G. Harding, "Bacteria and wound healing Colonisation Contamination," *Curr Opin. Infect. Dis.*, vol. 17, no. February, pp. 91–96, 2004.
 - [39] R. Podschun and U. Ullmann, "Klebsiella spp . as Nosocomial Pathogens : Epidemiology , Taxonomy , Typing Methods , and Pathogenicity Factors Klebsiella spp . as Nosocomial Pathogens : Epidemiology , Taxonomy , Typing Methods , and Pathogenicity Factors," *J. Clin. Microbiol.*, vol. 11, no. 4, pp. 589–603, 1998.
 - [40] S. Nagabhooshana, V. R. Vollala, and V. Rodrigues, "1 * , 2 , 1 1:," *Management*, vol. 2008, no. June, pp. 492–497, 2008.
 - [41] J. S. Boateng, K. H. Matthews, H. N. E. Stevens, and G. M. Eccleston, "Wound healing dressings and drug delivery systems: A review," *J. Pharm. Sci.*, vol. 97, no. 8, pp. 2892–2923, 2008.

- [42] V. S. S. Gonçalves *et al.*, "Alginate-based hybrid aerogel microparticles for mucosal drug delivery," *Eur. J. Pharm. Biopharm.*, vol. 107, pp. 160–170, 2016.
- [43] Food and Drug Administration, HHS, "Medical devices; general and plastic surgery devices; classification of tissue adhesive with adjunct wound closure device intended for topical approximation of skin. Final rule," *Fed. Regist.*, 2010.
- [44] F. SABRI, "Cell Growth apparatus and use of aerogels for directed cell growth," 2010.
- [45] M. T. Yen, J. H. Yang, and J. L. Mau, "Physicochemical characterization of chitin and chitosan from crab shells," *Carbohydr. Polym.*, vol. 75, no. 1, pp. 15–21, 2009.
- [46] I. R. Sweeney, M. Miraftab, and G. Collyer, "Absorbent alginate fibres modified with hydrolysed chitosan for wound care dressings - II. Pilot scale development," *Carbohydr. Polym.*, vol. 102, no. 1, pp. 920–927, 2014.
- [47] W. Li, J. Zhou, and Y. Xu, "Study of the in vitro cytotoxicity testing of medical devices (Review)," *Biomed. Reports*, pp. 617–620, 2015.
- [48] C. C. Liang, A. Y. Park, and J. L. Guan, "In vitro scratch assay: A convenient and inexpensive method for analysis of cell migration in vitro," *Nat. Protoc.*, vol. 2, no. 2, pp. 329–333, 2007.
- [49] The Clinical and Laboratory Standards Institute, *Performance Standards for Antimicrobial Susceptibility Testing CLSI supplement M100S*. 2016.
- [50] AATCC American Association of Textile Chemists and Colorists AATCC, *AATCC - Technical Manual*. 2016.
- [51] CLSI, *Methods for Dilution Antimicrobial Susceptibility Tests for Bacteria That Grow Aerobically*, no. January. 2015.
- [52] V. S. S. Gonçalves *et al.*, "Novel alginate-chitosan aerogel fibers for potential wound healing applications," *Pharm Anal Acta* 2016, 2016.
- [53] D. J. Dempsey and R. R. Thirucote, "Sterilization of medical devices: a review," *J. Biomater. Appl.*, vol. 3, pp. 454–523, 1989.
- [54] H. Tominaga *et al.*, "A water-soluble tetrazolium salt useful for colorimetric cell viability assay," *Anal. Commun.*, vol. 36, no. 2, pp. 47–50, 1999.
- [55] N. Balekar, N. G. Katkam, T. Nakpheng, K. Jehtae, and T. Srichana, "Evaluation of the wound healing potential of Wedelia trilobata (L.) leaves," *J. Ethnopharmacol.*, vol. 141, no. 3, pp. 817–824, 2012.
- [56] M. N. M. Walter, K. T. Wright, H. R. Fuller, S. MacNeil, and W. E. B. Johnson, "Mesenchymal stem cell-conditioned medium accelerates skin wound healing: An in vitro study of fibroblast and keratinocyte scratch assays," *Exp. Cell Res.*, vol. 316, no. 7, pp. 1271–1281, 2010.
- [57] C. Valgas, S. Machado de Souza, E. F. A Smânia, and A. Smânia Jr, "Screening Methods To Determine Antibacterial Activity of Natural Products," *Brazilian J. Microbiol.*, vol. 38, pp. 369–380, 2007.
- [58] N. Xing, F. Tian, J. Yang, and Y. K. Li, "Preparation and Basic Characterizations of Alginate-Chitosan Hydrogel," *Adv. Mater. Res.*, vol. 490–495, pp. 3396–3400, 2012.
- [59] W. P. Voo, B. B. Lee, A. Idris, A. Islam, B. T. Tey, and E. S. Chan, "Production of ultra-high concentration calcium alginate beads with prolonged dissolution profile," *RSC Adv.*, vol. 5, no. 46, pp. 36687–36695, 2015.
- [60] H. J. Kim *et al.*, "Polyelectrolyte complex composed of chitosan and sodium alginate for wound dressing application)," *J. Biomater. Sci. Polym. Ed.*, vol. 10, no. 5, pp. 543–556, 1999.
- [61] X. Shao and C. Hunter, *Developing an alginate/chitosan hybrid fiber scaffold for annulus fibrosus cells*, vol. 82A. 2007.
- [62] C. Wiegand, T. Heinze, and U. C. Hipler, "Comparative in vitro study on cytotoxicity, antimicrobial activity, and binding capacity for pathophysiological factors in chronic

- wounds of alginate and silver-containing alginate," *Wound Repair Regen.*, vol. 17, no. 4, pp. 511–521, 2009.
- [63] M. Huang, E. Khor, and L. Y. Lim, "Uptake and Cytotoxicity of Chitosan Molecules and Nanoparticles: Effects of Molecular Weight and Degree of Deacetylation," *Pharm. Res.*, vol. 21, no. 2, pp. 344–353, 2004.
 - [64] C. J. Knill *et al.*, "Alginate fibres modified with unhydrolysed and hydrolysed chitosans for wound dressings," *Carbohydr. Polym.*, vol. 55, no. 1, pp. 65–76, 2004.
 - [65] M. C. Straccia, G. G. D'Ayala, I. Romano, A. Oliva, and P. Laurienzo, "Alginate hydrogels coated with chitosan for wound dressing," *Mar. Drugs*, vol. 13, no. 5, pp. 2890–2908, 2015.
 - [66] L. Y. Zheng and J. F. Zhu, "Study on antimicrobial activity of chitosan with different molecular weights," *Carbohydr. Polym.*, vol. 54, no. 4, pp. 527–530, 2003.
 - [67] I. Smirnova, "Pharmaceutical Applications of Aerogels," in *Aerogels Handbook*, New York, NY: Springer New York, 2011, pp. 695–717.
 - [68] D. Kulig, A. Zimoch-Korzycka, A. Jarmoluk, and K. Marycz, "Study on alginate-chitosan complex formed with different polymers ratio," *Polymers (Basel)*, vol. 8, no. 5, pp. 1–17, 2016.
 - [69] G. F. Caetano *et al.*, "Chitosan-alginate membranes accelerate wound healing," *J. Biomed. Mater. Res. - Part B Appl. Biomater.*, vol. 103, no. 5, pp. 1013–1022, 2015.
 - [70] L. Wang, E. Khor, A. Wee, and L. Y. Lim, "Chitosan-alginate PEC membrane as a wound dressing: Assessment of incisional wound healing," *J. Biomed. Mater. Res.*, vol. 63, no. 5, pp. 610–618, 2002.